Chapter 1

Summary: Understand and simulate scale interactions (Catherine Rio and Frédéric Hourdin)

In the present book, we have described small-scale atmospheric phenomena, including convection, clouds, gravity waves

1.1 Introduction: Scale interactions in the atmosphere

The atmospheric circulation involves a whole ~~spectra~~ spectrum of scales, going from small scale turbulence (1-100 m, 10-600 s) that one can fill as gusts at the surface, to thermals organized motions (1 km), cumulus clouds (1-5 km), cumulonimbus (10-20 km) that may ~~organized~~ organize into meso-scale system (100-300 km), cyclones (500-1000 km), up to the global atmospheric circulation with its Rossby waves or Hadley-Walker circulation (1000-5000 km). Because the Navier-Stokes equations of fluid dynamics are non linear, those scales can not be considered ~~independently one from the~~ independent from each other. Understanding those interactions and modeling them is one of the most prominent and fascinating issue of atmospheric or oceanic physics. There is however generally no clear cut between the various scales which makes the question even more challenging.

The arrival of computers has been essential to make progress in the understanding and simulation of those scale interactions. Among the hierarchy of numerical models which have been developed through times~~in this view~~, the General Circulations Models (GCM) have proven to be a particularly powerful framework to understand these scale interactions and their role in the climate system. Manabe's Nobel prize for a large part recognized this major step in physics ~~(Manabe *et al.* 1965)~~(Manabe *et al.* 1965).

In GCMs, a fundamental and arbitrary separation is made between a ~~"larger scale"~~ large-scale flow (that of the synoptic structures of meteorological systems), explicitly represented in the model through a discretized ~~(or sometimes spectral)~~ formulation of the fluid mechanics equations, and sub-grid scale "parameterizations" of turbulent and convective motions, down to the scale of microphysics involved in particular in the formation of clouds and rainfall. This scale separation is illustrated in Fig. 1.1. With the increase of computational power through decades, it has become possible to run simulations at much finer scales on limited domain and time periods, with grid cells of the order of a few tens of meters. In these so-called Large Eddy Simulations (LES), a large part of the turbulent and convective motions are explicitly simulated. It is assumed that the remaining un-resolved motions are random, small scale and not too far from isotropy and can be well represented with a local turbulent diffusion approach. Formalizing what happens in those explicit simulations through conceptual models turned into parameterizations for global models, accounting for the coupling with radiation, large-scale atmospheric dynamics, land surface

processes or oceanic circulations, is one of the most sensitive aspect of climate modeling. It at the same time provides a fruitful avenue to the understanding of scale interactions.

In the present chapter, we try to present first the general formalism of the scale separation at the basis of GCMs (Section 2). Then we review the various approaches developed since the beginning of GCMs history for the parameterization of convection (section 3). We finally illustrate how this framework can be used to understand the scale interactions both locally and at global scale (section 4), before concluding on the key role of parameterizations to understand and simulate scale interactions (section 5). While Section 2 and 3 are very general and applicable to any GCM, the illustrations in Section 4 are made from one particular GCM, the LMDZ model, which is the atmospheric component of the IPSL coupled model IPSL-CM ~~(Boucher *et al.* 2020)~~ (Boucher *et al.* 2020) used in particular for climate change projections ~~in advance to~~ used in the IPCC assesment reports.

1.2 The general circulation model framework

In this first part, we briefly remind the scale decomposition at the basis of GCMs structure and introduce how parameterizations aim to represent sub-grid scale physical processes and their interactions with the large-scale flow.

1.2.1 Conservation laws and Reynolds decomposition

General circulation models rely on the Reynolds decomposition to separate the flow between scales which are "explicitely resolved" given the grid cell size of a model and "subgrid-scale motions". The Reynolds decomposition however has a scope far beyond grid point models.

Let us consider any scalar quantity ~~$q(\vec{x},t)$~~ $\phi(\vec{x},t)$ transported by the air (where $\vec{x}$ stands for the location in space and t for time), associated with velocity field $\boldsymbol{v}(\vec{x},t)$ and air density $\rho(\vec{x},t)$, related by the continuity equation

$$\frac{\partial \rho}{\partial t} + \boldsymbol{\nabla} \cdot \rho \boldsymbol{v} = 0 \tag{1.1}$$

The conservation of ~~q~~ ϕ can be written as

$$\frac{Dq}{Dt} \frac{D\phi}{Dt} = S_\phi \quad \text{Lagrangian derivative along air trajectories} \text{~~+=Advective form+}\rho\text{= }\rho\text{flux form} \tag{1.2}$$

which, using the continuity equation, can be expressed equivalently in advective or flux forms:

$$\frac{\partial \phi}{\partial t} + \boldsymbol{v} \cdot \boldsymbol{\nabla} \phi = S_\phi \quad \text{Advective form} \tag{1.3}$$

$$\frac{\partial \rho\phi}{\partial t} + \boldsymbol{\nabla} \cdot \rho \boldsymbol{v} \phi = \rho S_\phi \quad \text{Flux form} \tag{1.4}$$

where S_ϕ is a source of tracer (chemical reaction, water phase change, heating for potential temperature, ...).

The Reynolds decomposition considers the flow as a random process. In this decomposition the large scale is considered as the statistical expectation $\widetilde{X(\vec{x},t)}$ of a random realisation of the flow $X_i(\vec{x},t)$ both defined at each point in space and time.

For a compressible fluid, one should introduce a weighted average, by the air density : ~~$\overline{X} = \widetilde{\rho X}/\widetilde{\rho}$.~~

$$\overline{X} = \widetilde{\rho X}/\widetilde{\rho} \tag{1.5}$$

The turbulent fluctuations with respect to this air weighted average $X' = X - \overline{X}$ obey $\widetilde{\rho X'} = \overline{X'\widetilde{\rho}} = 0$ (as can be easily seen from Eq. 1.5). Taking the ensemble mean of the flux form of the conservation of ~~q (ϕ~~ (Eq. 1.4) and through simple algebra, it ~~comes~~ becomes

$$\frac{\partial \left(\widetilde{\rho}\ \overline{\phi}\right)}{\partial t} + \boldsymbol{\nabla} \cdot \left(\widetilde{\rho}\ \overline{\boldsymbol{v}}\ \overline{\phi}\right) + \boldsymbol{\nabla} \cdot \left(\widetilde{\rho}\ \overline{\boldsymbol{v}'\phi'}\right) = \widetilde{\rho}\ \overline{S_\phi} \tag{1.6}$$

Using notation $\rho \equiv \widetilde{\rho}$, $\boldsymbol{v} \equiv \overline{\boldsymbol{v}}$ et ~~$c \equiv \overline{c}$~~ $q \equiv \overline{q}$ for the large scale variables, the conservation (Eq. 1.2, 1.3, 1.4) are formally unchanged if adding

$$S_\phi^* = -\frac{1}{\rho}\boldsymbol{\nabla} \cdot \rho\overline{\boldsymbol{v}'\phi'} \tag{1.7}$$

to the source term S_ϕ. S_ϕ^* is a local source for the quantity ~~q~~ ϕ resulting from the effect of unresolved (or sub-grid scale, or turbulent, or convective) motions on the large sale variables. ~~$F_q = \rho\overline{\boldsymbol{v}'q'}$~~ $F_\phi = \rho\overline{\boldsymbol{v}'\phi'}$ is the turbulent flux of ~~$q\phi$~~, which is non zero only if the fluctuations of $\boldsymbol{v}$ and ~~q~~ ϕ are correlated. For convection or turbulence, the fluctuations of $\boldsymbol{v}$ drives fluctuations of ~~q~~ ϕ and the resulting flux are most often non zero.

~~Note that the ensemble average is required as a concept to define the large scale variables in the Reynolds decomposition, rather than a simpler spatial or temporal running mean, because only the ensemble mean permutes mathematically with both temporal and space derivatives in the equations. The idea behind is that these three averages are equivalent in theory thanks to the ergodicity of the atmospheric flow.~~ [1]

The decomposition can be used to account for the effect of small turbulent scales (~~-~~1-100 m) on the organized motions in a convective cloud for instance (~~-~~0.5~~-10km~~-10 km), as done in Large Eddy simulations (not meaning that there is a clear gap between those scales in the energy spectrum).

It can be used at larger scale to account for the effect of all the turbulent and convective processes (~~-1m-10km~~1m-10 km) on the circulation at synoptic scale, that of weather systems (500-5000 km). The gap between those two scales is often well marked but not always (fronts, meso-scale organized storms, cyclones).

It is this last separation which is done in General Circulation Models. Because of the stratification of the flow by gravity, the grid cells are extremely elongated horizontally, with horizontal dimension of typically 30-300 km and typical vertical extension of 10 m (close to the surface) to 200 m to 2 km in the free troposphere. The parameterizations that represent the processes in the GCM framework assume ~~an~~ horizontal homogeneity of the processes involved. The turbulence or the cloud size may have a complex spectrum, but the moments of this spectrum does not vary horizontally within the grid cell. When assuming horizontal homogeneity of the statistical distribution of subgrid scale processes, all the transfer equations reduce to 1D on the vertical and the Reynold source term reduces to:

$$S_\phi^* = -\frac{1}{\rho}\frac{\partial \rho\overline{w'\phi'}}{\partial z} \tag{1.9}$$

An illustration of the scale-separation done in GCM between a 3D representation of the large scale circulation and parameterizations of vertical transfers is given in Fig. 1.1.

1.2.2 Primitive equations of meteorology with source terms

The General Circulation Models are based on the so-called primitive ~~equation~~ equations of meteorology, a modified version of the Navier-Stokes equations, in which the vertical component of the

[1] Note that the ensemble average is required as a concept to define the large scale variables in the Reynolds decomposition, rather than a simpler spatial or temporal running mean, because only the ensemble mean permutes mathematically with both temporal and space derivatives in the equations. For instance a running mean in time

$$\widetilde{X(x,t)} = \frac{1}{T}\int_{t-T/2}^{t+T/2} X(x,t')dt' \tag{1.8}$$

The idea behind is that these three averages are equivalent in theory thanks to the ergodicity of the atmospheric flow.

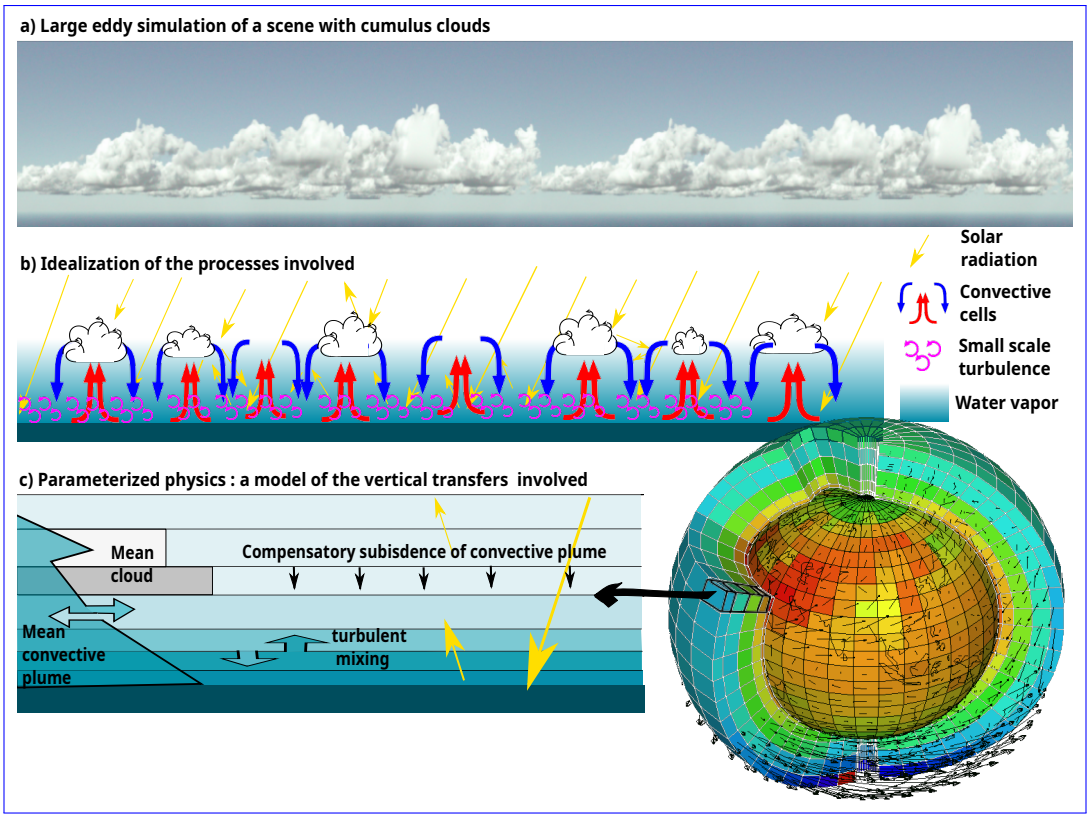

Figure 1.1: Idealized view of the separation done in GCMs to model the scale interaction between local processes (here turbulence, boundary layer convection and clouds) and the large scale circulation explicitly represented through a global 3D discretized version of the 3D primitive equations of meteorology. The three horizontal panels represent : a) a picture of a large eddy simulation of a case of shallow cumulus (the ARM case) run ~~with an LES~~ at 8 m resolution on a domain of 12 km^2. Everything is physical in this picture including the rendering which is done with a ray-tracing approach ~~(Villefranque *et al.* 2021)~~(Villefranque *et al.* 2021). The picture is duplicated twice horizontally to give a better idea of the aspect ratio which is targeted in GCM parameterizations; b) idealisation of the processes at work in such a scene, with small scale turbulence, organized convective structures of the boundary layer, and clouds; c) a schematic view of the way those processes are handled with the eddy-diffusivity mass-flux parameterization approach. The small scale turbulence mixes air between adjacent layers while the mass flux scheme transports directly the air from the lower layers to the upper part of the boundary layer with some lateral mixing and a compensatory subsidence, generally much weaker and occurring on a larger horizontal fraction of the grid. A mean cloud is also parameterized ~~which~~ whose properties interact with radiation.

momentum equation is replaced by the hydrostatic equilibrium (typically valid at horizontal scales larger than 10 km, see chapter 9 of book A) and the vertical variation of the horizontal distances is neglected, considering that the depth of the atmosphere is small compared to the planetary radius. The primitive equations (see chapter 4 of book A) with source terms read

$$\frac{D\boldsymbol{v}_h}{Dt} + 2f\boldsymbol{k}\times\boldsymbol{v}_h + \frac{1}{\rho}\mathrm{grad}\boldsymbol{\nabla}p = -\frac{1}{\rho}\frac{\partial\rho\overline{w'\boldsymbol{v}'_h}}{\partial z} = Q_3\boldsymbol{Q_3} \tag{1.10}$$

$$c_p\frac{D\theta}{Dt} = Q_R + L_v(c-e) - \frac{1}{\rho}\frac{\partial\rho\overline{w'\theta'}}{\partial z} = Q_R + Q_1 \tag{1.11}$$

$$\frac{Dq_v}{Dt} = e - c - \frac{1}{\rho}\frac{\partial\rho\overline{w'q'_v}}{\partial z} = -Q_2/L_v \tag{1.12}$$

$$\frac{Dq_c}{Dt} = c - e - \frac{1}{\rho}\frac{\partial\rho\overline{w'q'_c}}{\partial z} \tag{1.13}$$

where $\boldsymbol{v}_h = (u, v, 0)$ is the 'horizontal' component of the velocity, $f = 2\Omega\sin\varphi$ is the Coriolis parameter, $\phi = gz$ is the geopotential, θ is the potential temperature, q_v and q_c are the mixing ratio of vapor and condensed water (for the sake of simplicity, the distinction between ice and liquid water will not be made here although it is important in some cases), Q_R is the heating by radiation, c and e the condensation and evaporation of water, L_v the associated latent heat constant.

Notations Q_1, Q_2 were introduced historically by ~~(Yanai *et al.* 1973)~~ Yanai *et al.* (1973) to determine the bulk properties of tropical cloud clusters from large-scale heat and moisture budgets. They represent respectively the "apparent" source of heat and sink of water vapor expressed as a sink of energy. ~~Q_3~~ $\boldsymbol{Q_3}$ stands for the apparent source of horizontal momentum. Estimating those terms is the purpose of parameterizations.

Beyond its success in weather forecast and climate change anticipation, the framework of General circulation models convey a fundamental idea that governs much of our thinking on how scales interact in meteorology and climate: the large scale motions organize essentially horizontally, within a thin layer above the earth surface, the large scale subsiding or ascending motions balancing the horizontal divergence of these horizontal motions. Turbulent or convective transport, radiative heating, or condensation/evaporation of water interact with those large scales locally through vertical transfers (plus heat, moisture and momentum fluxes at the surface and radiative exchange with space).

As any model, this GCM framework has its own limitations. Assuming that turbulence or convection is statistically homogeneous horizontally is an approximation which may not be verified occasionally at any horizontal scale between a few hundreds of meters and a few hundreds of km depending on the meteorological situation. However, the gain in both numerical cost and understanding compared to a full simulation of all the convective motions (as targeted in LES) is huge. It can be compared to the gain made when using Navier-Stokes rather than Boltzmann description for a fluid. It justifies to put energy in developing and improving convective parameterizations and pushing them to try to compensate for the intrinsic limitations of the GCM framework.

1.2.3 The world of parameterizations

Parameterizations are based upon a (conceptual) model (an idealization) of the process to be represented and of its coupling with the local large scale environment. Starting from the vertical profile of the GCM state variables, $X = (\boldsymbol{v}_h, \theta, q_v, q_c)$, internal variables Y are generally derived, such as a mixing length for turbulence, a vertical velocity in convective plumes, a fractional cover by clouds, etc. Combining both the GCM state variables and internal variables, a term Q_x (a contribution to $Q_{1,2,3}$) is finally computed and used as a source terms for the primitive equations.

In the most restrictive framework, the internal variables directly depend on the large-scale variables through a closure relationship, $Q_x = F(X, \lambda)$, where λ is a vector of free parameters that enter in the parameterization.

The most classical example of such parameterization is the local eddy-diffusion. The underlying image is that small turbulent motions mix quantities similarly to the way ~~brownian~~ Brownian motions mix quantities in a fluid. The vertical turbulent flux is proportional, with a negative coefficient, to the vertical gradient of the transported quantity $\overline{\rho w' q'} = -\rho K_z \frac{\partial q}{\partial z}$ $\overline{\varrho w' \phi'} = -\varrho K_z \frac{\partial \phi}{\partial z}$. For an isotropic turbulence, typically in a neutral atmosphere, and introducing a mixing length l ~~caracteristic~~ characteristic of the eddies, one obtains $K_z = l^2 ||\partial \boldsymbol{v}_h / \partial z||$. If the atmosphere is non neutral, the coefficient could be corrected as a function of the Richardson number (defined in chapter **??**) which itself depends on the vertical profile of the model state variables.

However, this formalism fundamentally assumes that a quasi steady state regime is reached at any time between the sub-grid scale processes and large scale state variables vertical profiles. In practice, in many recent parameterizations, some internal variables of the parameterizations follow their own time evolution:

$$Q_x = F(X, Y, \lambda_F) \tag{1.14}$$

$$\frac{\partial Y}{\partial t} = G(X, Y, \lambda_G) \tag{1.15}$$

λ_F and λ_G being the subset of the free parameters that enter in each equation. This is typically the case of state-of-the-art turbulent schemes in which a prognostic equation of turbulent kinetic energy ~~$TKE = \frac{1}{2}\overline{u'^2 + v'^2 + w'^2}$~~ $TKE = \frac{1}{2}(\overline{u'^2 + v'^2 + w'^2})$ is introduced to derive the eddy diffusivity $K_z = lS\sqrt{TKE}$ where l is a turbulent mixing length and S a stability function (generally themselves object of parameterizations). In theory and sometimes in practice, the computation of the time evolution of Y also ~~account~~ accounts for the effect of large scale advection.

The parameterizations also sometimes interact with each other ; the time evolution of the state variable Y_2 of parameterization P2 may depend directly upon the internal state variables Y_1 of parameterization P1. For instance, as will be illustrated latter on, the triggering of deep convection in a model may depend not only on the stability of the atmosphere but also on the characteristics of shallow convection, as provided by an other parameterization; similarly, the specification of the horizontal sub-grid scale distribution of cloud water, used to compute the cloud fraction as the fraction of the grid cell above saturation, can depend upon the convective mass fluxes computed in a convective parameterization. The cloud fraction is then used to compute the radiation or the conversion of condensed water to rainfall.

Compromises must be made as concerns the complexity of the parameterizations and their couplings. ~~However~~Even if parameterizations are simplifications of real processes, each time a sophistication of the models underlying convective parameterizations improves the behaviour of the climate model, a step is made in the understanding of the scale interaction between the convection and large scale circulation.

1.2.4 Parameterization development and sensitivity experiments

Development of parameterizations is generally a mix of some fundamental principles (conservation of energy, water, momentum) with a heuristic view of the way the small scale motions emerge and organize. This view can come from rather well established equations, like in the turbulent closures based on the turbulent kinetic equations for ~~small scale~~ small-scale turbulence, which are quite general and ~~well founded~~well-founded, and could in theory be applied on any planetary environment. When trying to summarize the complexity of cloud and convective organization into parameterizations, one has to make choices, prioritize ~~process~~ processes that matter, decide to unify for instance dry and cloudy shallow convection, or shallow and deep convection, or other options. And it is very important that different choices are tested in different teams because no choice is fully satisfying and because such parameterization can not be purely derived from first principles.

Because they are approximations of complex processes, parameterizations include adjustable parameters, which may be well-constrained by observations or be highly uncertain, and depend on the sophistication of the parameterization. It could be the diffusion coefficient K_z or a parameter

used in the formulation of the mixing length used to compute this coefficient; it could be the mean radius of cloud droplets assumed to be ~~the~~ uniform over the planet, or parameters in a parametrization of microphysics attempting to compute droplet radius.

Developing a parameterization consists in proposing functions F and G, and their discretized forms, as well as fixing the values of free parameters λ_F and λ_G. A now classical approach in parameterization development for convection and clouds consists in comparing the results produced by the parameterizations within a single column of the model (SCM) with either observations or high resolution LES that explicitly resolve the processes targeted by the parameterization. The idea is illustrated in Fig. 1.1. Depending on the parameterization choices and value of free parameters, the "climate" (statistics done on simulated trajectories) simulated by the full 3D will differ. Some choices may produce a climate too far from observation to be of any use for any purpose. A very important step to obtain usable model configurations consists in calibrating or tuning the values of the model free parameters, in order to guarantee some important properties. One key issue is the calibration of cloud parameters, which are the most uncertain ~~that~~ and which affect radiation that drives the atmospheric circulation at large scale. Model calibration was rather recently recognized as a key aspect of climate modeling ~~(?)~~ (Hourdin *et al.* 2017) and recent machine learning techniques ~~(?)~~ (?) are more and more used for this calibration. A first phase of calibration can be done comparing LES with single column simulations (as explained above) before tuning the full global model ~~(Couvreux *et al.* 2021 ; Hourdin *et al.* 2021)~~(Couvreux *et al.* 2021 ; Hourdin *et al.* 2021).

Two different questions emerge when developing parameterizations, that will be illustrated in the rest of this chapter by focusing on the convection process. The first one concerns the way the large scale atmospheric conditions affect the statistics of the smaller scale motions, ~~ie~~ i.e. deducing Y and Q_x knowing X. This will be the subject of Section 3. The second one, addressed in section 4, concerns the way sub-grid scale processes affect locally the environment and then the large scales of the meteorology and climate. The separation done in GCMs is very useful to address this question, since it allows to test how a change in Q_x affects the large scale. This can be done by running sensitivity tests modifying the atmospheric parameterizations (F or G or the value of the free parameters).

1.3 Parameterizing convective processes

Convective processes result from a destabilization of the atmospheric column. One distinguishes on the one hand shallow convection with a vertical extension of a few kilometers and typical vertical velocity of 1-2 m/s. Shallow convection occurs even in the absence of clouds (dry convection) and leads to the formation of stratocumulus and cumulus clouds. Deep convection on the other hand, associated with cumulonimbus clouds, very often reaches the tropopause (~10-15 km) with vertical motions that reach several tens of m/s. In-between, congestus clouds are precipitating clouds that usually stop around the freezing level.

The purpose of a convective parameterization is to summarize the collective effect of an ensemble of convective motions (or cells, or clouds) of various sizes on its environment without describing each individual motion. A parameterization of convection should provide a contribution to the source terms (~~Q1, Q2, Q3~~Q_1, Q_2, $\boldsymbol{Q_3}$) of the dynamical equations as well as a source term associated to the convective transport of trace species other than water. It should also provide the precipitation rate for cloudy convection and eventually macro and microphysical properties of associated clouds for radiation.

It should not only be valid over the broadest possible range of conditions, but also respond appropriately to changes in natural forcing ~~(Raymond 1994). To achieve this, it is noteworthy~~ (Raymond 1994). This requires to take into account the main processes driving convection initiation and life cycle as sketched in Fig. 1.2. Those processes are discussed hereafter.

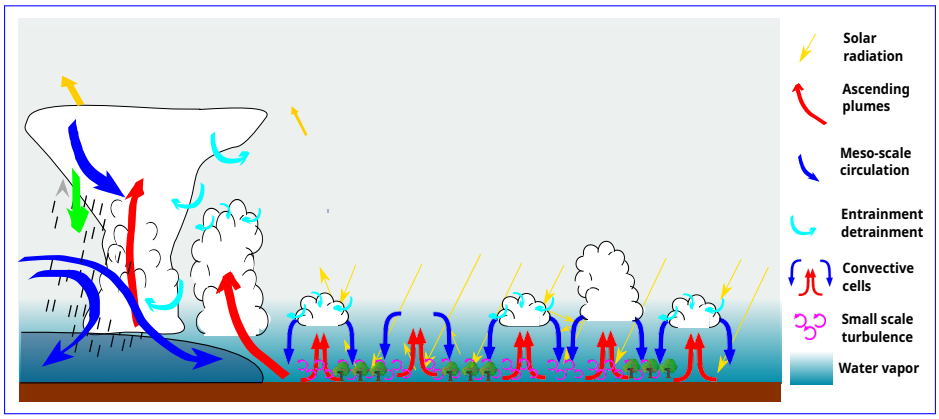

Figure 1.2: Physical processes to be parameterized to represent convection and its interaction with the large-scale: convective-scale updrafts and downdrafts associated with dry, shallow or deep convection; mixing between convective updrafts and its environment; condensation and precipitation, which evaporation leads to the formation of cold pools spreading at the surface; mesoscale updrafts and downdrafts.

1.3.1 A brief history of convective parameterization

As explained by Arakawa in his review of convective parameterizations ~~(Arakawa 2004)~~(Arakawa 2004) , first attempts to parameterize cumulus convection (shallow or deep) have given rise to two schools of thought:
- Convection acts against the destabilization of the atmosphere ~~that created it~~ via an adjustment: "the adjustment school" ~~(Manabe *et al.* 1965)~~(Manabe *et al.* 1965).
- Convection is controlled by the large-scale convergence of warm and moist air in a surface layer, "the convergence school" ~~(Ooyama 1964)~~(Ooyama 1964).

Those first approaches attempted to represent the interactions between convection and the large-scale without representing the mean properties of underlying convective processes explicitly.

In the early 70s, the so-called mass-flux approach was proposed to relate the source terms (Q_1, Q_2, Q_3) ~~(Q_1, Q_2, Q_3)~~ to convective updraft properties, in both observational ~~(Yanai *et al.* 1973) and modelling (Arakawa and Schubert 1974)~~ (Yanai *et al.* 1973) and modelling (Arakawa and Schubert 1974) studies. This approach depicts convection as an ensemble of updrafts and downdrafts occurring within the same model column. The first parameterizations of convection represented shallow cloudy convection (cumulus) in conjunction with deep convection (cumulonimbus), by considering a ~~spectra~~ spectrum of convective clouds entraining environmental air at different rates ~~(Arakawa and Schubert 1974)~~(Arakawa and Schubert 1974). Several mass-flux schemes were developed based on this framewok in the 80s and 90s ~~(Tiedtke 1989 ; Emanuel 1991 ; Del Genio and Yao 1993 ; Kain and Fr~~ (Tiedtke 1989 ; Emanuel 1991 ; Del Genio and Yao 1993 ; Kain and Fritsch 1993) leading to a variety of parameterizations meant to represent both shallow and deep convection initiated at cloud base and differing by their internal hypothesis to represent the main processes driving convection illustrated in Fig. 1.2.

In parallel, an often distinct literature emphasized the need to break from local formulations of the vertical turbulent transport in the boundary layer. In particular, ~~(Deardorff 1966)~~ Deardorff (1966) first insisted on the fundamental impossibility for eddy-diffusion to transport heat upward in a neutral or slightly stable atmosphere, a situation almost systematically observed in the convective boundary layer. This literature rather favors parameterizing both clear and cloudy shallow convection as part of the boundary-layer processes, cumulus clouds being seen as the saturated part of buoyant thermal plumes initiated at the surface, as documented in observations by ~~(LeMone and Pennell 1976)~~LeMone and Pennell (1976).

Various propositions were made to break from the local view of boundary layer transport by diffusion, either by adding a counter gradient term ~~(Deardorff 1966 ; Troen and Mahrt 1986 ; Holtslag and Boville 1993)~~

(Deardorff 1966 ; Troen and Mahrt 1986), introducing new concepts as transilient matrices (Stull 1984 ; Pleim and Xiu 1
(Stull 1984) or using higher order moment turbulent closure (Abdella and McFarlane 1997 ; Lappen and Randall 2001 ; I
(Larson and Golaz 2005). The combination of a mass flux scheme representing the organized structure of the convective boundary layer with eddy diffusivity was first proposed by (Chatfield and Brost 1987)
Chatfield and Brost (1987). The resulting Eddy Diffusivity - Mass Flux formalism (Hourdin *et al.* 2002 ; Soares *et al.* 200
(Hourdin *et al.* 2002 ; Siebesma *et al.* 2007), which combines a mass flux representation of the convection with eddy diffusivity, is one of those approaches, which is now used routinely both in climate models with coarse horizontal grid cells (Rio and Hourdin 2008 ; ?) (Rio and Hourdin 2008) or numerical weather forecast models (Pergaud *et al.* 2009) (Pergaud *et al.* 2009) at kilometric resolution. In this approach, shallow convection is handled in conjunction with cloud free convective boundary layer rather than with deep convection.

The question of separating or unifying the parameterization of shallow and deep convection is at the heart of the research in that field (Rio *et al.* 2019). If some development teams approaches target to unifying the parameterization of shallow and deep convection(Park 2014 ; Suselj *et al.* 2019) , separating scales in different parameterizations offers the possibility to study scale interactions by considering their interplay as will be shown in Section 1.4.

1.3.2 The mass-flux approach

The now widely used mass-flux approach for parametrizing convection consists in decomposing a column of the GCM, typically from 30 to 300 km wide, into different compartments or sub-columns associated with organized vertical motions. One compartment, associated with a unique vertical velocity profile, may correspond to the parameterization of a mean ascending plume, or several compartments may be attributed to the convective ascent to represent a spectrum of vertical motions. In presence of rainfall, the representation of a precipitating downdraft as a separate compartment is added ; all the mass flux parameterizations include a distinct compartment for a compensating subsidence (in order to insure that the total mass flux is null in the parameterisation, $\widetilde{\rho}\overline{w'} = 0$, as required by the Reynolds decomposition). In each of the compartments, a mass flux $\rho w'$ is computed (parameterized) and use used to transport conserved quantities.

In the most simple case, the column is separated between one ascending convective plume covering a fraction α_u, and the environment covering a fraction $\alpha_e = 1 - \alpha_u$, in which a slow compensating subsidence occurs. Then, the mean of a quantity q ϕ can be expressed as:

$$\overline{\phi} = \alpha_u \overline{\phi}^u + \alpha_e \overline{\phi}^e \tag{1.16}$$

where subscript u stands for the updraft and subscript e stands for the environment.

As the flux of the quantity q ϕ is given by:

$$\overline{w'\phi'} = \overline{w\phi} - \overline{w}\ \overline{\phi} \tag{1.17}$$

we have:

$$\overline{w'\phi'} = \alpha_u \overline{w\phi}^u + \alpha_e \overline{w\phi}^e - (\alpha_u \overline{w}^u + \alpha_e \overline{w}^e)(\alpha_u \overline{\phi}^u + \alpha_e \overline{\phi}^e) \tag{1.18}$$

Considering that $\overline{wq}^u = \overline{w'q'}^u + \overline{w}\ \overline{q}$ and $\overline{wq}^e = \overline{w'q'}^e + \overline{w}\ \overline{q}$ $\overline{w\phi}^u = \overline{w'\phi'}^u + \overline{w}^u\ \overline{\phi}^u$ and $\overline{w\phi}^e = \overline{w'\phi'}^e + \overline{w}^e\ \overline{\phi}^e$ and developing Eq. 1.18 leads to:

$$\overline{w'\phi'} = \alpha_u \overline{w'\phi'}^u + \alpha_e \overline{w'\phi'}^e + \alpha_u \alpha_e (\overline{w}^u - \overline{w}^e)(\overline{\phi}^u - \overline{\phi}^e) \tag{1.19}$$

If one makes the hypothesis that the fraction covered by the updraft is small compared to the grid sizeand that the mean vertical velocity is zero: $\alpha_u << 1$, $\overline{w} = 0$ and $\overline{q}^e = \overline{q}$, then we further have $\overline{w}^e << \overline{w}^u$ and $\overline{\phi}^e = \overline{\phi}$, and the flux of q ϕ reduces to:

$$\overline{w'\phi'} = \alpha_u \overline{w'\phi'}^u + \alpha_e \overline{w'\phi'}^e + \alpha_u \overline{w}^u (\overline{\phi}^u - \overline{\phi}) \tag{1.20}$$

On the right-hand side, the first term corresponds to intra-structures turbulence which is neglected in common parametrizations, the second one to fluctuations within the environment

which is taken into account by the diffusion scheme mentioned previously, and the third one to the contribution of coherent ascending structures and their compensating subsidence within the environment. Defining the vertical mass-flux as $f_u = \alpha_u \rho w_u$ (to simplify notations, from now on, we denote averages over upward and downward areas with subscripts, e.g., $\overline{w}^u = w_u$), the mass-flux contribution to the turbulent flux of ~~q~~ ϕ is given by:

$$\rho \overline{w'\phi'} = f_u \times (q\phi_u - \overline{\phi}) \tag{1.21}$$

Then, deriving the turbulent flux associated with convection requires to compute the mass-flux and the updraft properties. Those can be derived by the conservation equations. The vertical transport of a state variable ~~q~~ ϕ of the model can be computed using the ~~stationnary~~ stationary plume conservation equation:

$$\frac{\partial f_u q_u}{\partial z} \frac{\partial f_u \phi_u}{\partial z} = e_u q \phi_e - d_u q \phi_u + \alpha_u \rho S_{q_u \phi_u} \tag{1.22}$$

e_u is the lateral entrainment rate of environmental air into the updraft and d_u is the lateral detrainment rate of updraft air into the environment. ~~S_{q_u}~~ S_{ϕ_u} stands for source terms regarding to the chosen variable ~~q~~ϕ:
- For variables conserved during an ~~adiabatically~~ adiabatic ascent, such as the liquid temperature θ_l or total humidty (vapor + condensates) q_t, ~~$S_{q_u} = 0$~~ $S_{\phi_u} = 0$,
- For a tracer equal to unity, ~~$S_{q_u} = 0$~~ $S_{\phi_u} = 0$, and Eq.1.22 yields to the equation of conservation of mass, often used to compute the mass flux f_u ~~form~~ from the entrainment and detrainment, e_u and d_u,
- For vertical momentum w_u, although more complete and well founded formulations exist ~~(Gregory 2001)~~ (Gregory 2001) the most classical formulation assumes that the source term (acceleration) is the sum of buoyancy and a drag term proportional to the square of the vertical velocity ~~(Simpson and Wiggert 1969)~~ ~~:~~ (Simpson and Wiggert 1969):

$$S_{\Phi_u w_u} = a_1 g \frac{\theta_{vu} - \theta_{ve}}{\theta_{ve}} - a_2 \epsilon w_u^2 \tag{1.23}$$

where θ_v is the virtual potential temperature and a_1 and a_2 are tunable parameters.

Additional equations are needed to compute the lateral entrainment and lateral detrainment rates and to initiate the updraft: in what environmental conditions does it form and with which intensity (mass-flux value at the ~~cloud base~~ base of the upadraft)? Those hypothesis are what differentiate the existing schemes and can be different depending on the convection type as will be described below.

1.3.3 Surface forcing and convective instability

The main driver of atmospheric convection is the excess of heat at the surface which results from solar radiation. About half of the time over the globe, the first few hundreds meters above surface ~~typically (~~ are typically (i.e. the surface boundary layer) ~~are~~ unconditionally unstable. This occurs in practice when the atmosphere is super adiabatic, ~~-~~i.e. when the potential temperature decreases with height (when the natural temperature decreases faster than 10 K/km). In such conditions, an air parcel displaced vertically will accelerate away from its original position, leading to strong vertical motions that organize in plumes, cells or rolls, with a strong analogy with Rayleigh Bénard experiments. The temperature decrease within the rising plume can lead to the formation of clouds above a given level if the air is moist enough at the surface.

In this cloudy layer, the atmosphere is called conditionally unstable: it is stable for unsaturated parcels whose lapse rate follows a dry adiabatic, and unstable for saturated parcels with a moist adiabatic lapse rate.

~~As introduced in chapter 2 (section 2.2), a positively buoyant air parcel rising from the surface follows a dry adiabat and its virtual potential temperature is constant until its lifting condensation~~

level, where it is negatively buoyant and eventually falls back down. When the heat released by condensation is enough to overcome a convective instability The mechanisms of deep convection introduced in chapter 2 (section 2.2), and the concepts of convective inhibition (CIN) barrier that most often prevails at the basis of cumlus clouds, the parcel may continue rising until its virtual potential temperature overcomes the one of the environment, at the level of free convection, and then rise up freely to the level where its virtual potential temperature equals the one of the environment, at the level of neutral buoyancy. The so called and convective available potential energy (CAPE) at a given level z is given by the integral of the parcel buoyancy between the level of free convection and the altitude z.

This simple parcel view allows allow to introduce two aspects fundamental to parameterize convection: the triggering, a criterion defining if there is convection or not (if a parcel rising from the surface is able to overcome the CIN); the closure which determines the intensity of the convection, which in turn will comsume the CAPE. One reason to parameterize shallow and deep convection separately is that the processes that predominantly control their triggering and closure are different.

Unified mass-flux scheme for dry and shallow convection are simply initiated at the surface in the presence of an instability and cumulus clouds form if there is condensation along the ascent. In this case, the vertical velocities in clear sky and cumulus topped boundary layers scale quite well with surface heat fluxes via the so-called convective velocity (Deardorff *et al.* 1970) (Deardorff *et al.* 1970) $w* = [\frac{g}{\theta} z_i \overline{w'\theta'_0}]^{\frac{1}{3}}$, where z_i is the height of the mixed layer and $\overline{w'\theta'_0}$ the surface heat flux, so that the closure relies convective intensity to the surface heat flux (Soares *et al.* 2004 ; Siebesma *et al.* 2007 ; Pergaud *et al.* 2009 ; Bretherton and Park 2009)(Soares *et al.* 2004 ; Brether . Differently, (Hourdin *et al.* 2002) Hourdin *et al.* (2002) considers a 2D circulation of convective rolls that scales the horizontal velocity of the air entrained within the thermal plume relates the horizontal convergence of mass in the surface layer with the maximum vertical velocity mass-flux within the plume to derive a mass-flux at the top of the surface layer.

In the case of deep convection, the conditions leading to the sudden burst of cumulonimbus clouds are less understood. Those include the moistening of the low troposphere by detrainment from cumulus clouds (Chaboureau *et al.* 2004)(Chaboureau *et al.* 2004), the lifting of air at the border of cold pools created by the evaporation of precipitation from congestus clouds (Khairoutdinov and Randall 2006)(Khairoutdinov and Randall 2006), or additional surface forcing linked to surface heterogeneities, orography or land-sea contrast (Rochetin *et al.* 2017 ; Harvey *et al.* 2022) (Rochetin *et al.* 2017 ; Harvey *et al.* 2022). The way of representing the triggering of deep convection is a challenge for parameterizations and may involve scale interactions between shallow and deep convection. Once initiated, deep convection generally overcomes the freezing level and rapidly reaches the tropopause, overshooting above the level of neutral buoyancy. Water phase changes and precipitation, of both liquid and ice, play a key role in the cumulonimbus evolution. Most parameterization of deep convection relate the convective intensity at cloud base to the CAPE, assuming a quasi-equilibrium between convection and the large-scale forcing. The convection tends to reduce the CAPE produced by the large-scale forcing over a specific timescale τ of the order of 1 hour. An other view is to relate convective intensity at cloud base to underlying boundary-layer properties: moisture convergence or vertical advection of moisture in the sub-cloud layer (Kuo 1965 ; Bougeault 1985)(Kuo 1965 ; Bougeault 1985), or an available lifting power provided by the dynamics of boundary-layer thermals and cold pools (Rio *et al.* 2013)(Rio *et al.* 2013).

1.3.4 Lateral mixing and sensitivity to tropospheric humidity

Tropospheric humidity plays a key role in the vertical extension of convective clouds (Derbyshire *et al.* 2004) . This is due to the mixing process between convective updrafts and environmental air. This mixing Combining Eq. ?? for a conserved variable and the equation for the conservation of mass yields:

$$\frac{\partial \phi_u}{\partial z} = \frac{e_u}{f_u}(\phi_e - \phi_u) \tag{1.24}$$

Then, the vertical evolution of the updraft properties directly depends on the lateral entrainment rate e_u. Entrainment will both dilute the updraft and may also change its buoyancy. In a very dry air, ~~the mixing~~ entrainment will strongly decrease the buoyancy of the updraft air parcels by evaporative cooling. ~~This mixing is described in the mass flux approach as the sum of lateral entrainment and detrainment.~~

~~Entrainment and detrainment are~~ Tropospheric humidity thus plays a key role in the vertical extension of convective clouds (Derbyshire *et al.* 2004). This entrainment rate is difficult to diagnose from observations~~and LES. Hence the first~~. First formulations were based on geometrical considerations, making entrainment inversely proportional to the updraft radius. ~~First formulations considered constant values of the fractional entrainment and detrainment rates, $\epsilon_u = e_u/f_u$ and $\delta_u = d_u/f_u$, issued from LES analysis in the case of shallow convection (Siebesma and Cuijpers 1995). Then, different~~ Several formulations have been proposed ~~based on different physical considerations. For example, (Neggers *et al.* 2002) formulates~~ overtime, based on LES studies (Siebesma and Cuijpers 1995), defining the fractional entrainment rate~~as being inversely proportional to the vertical velocity within the updraft ; (von Salzen and McFarlane 2002) defines it as proportional to the buoyancygradient; (Bechtold *et al.* 2008) relates it directly to~~ $\epsilon_u = e_u/f_u$ as a function of updraft properties (buoyancy, vertical velocity) or directly of the relative humidity of the environment ~~; while (Gregory 2001) defines it so that it reduces the acceleration due to buoyancy~~(see De Rooy *et al.* (2013) for a review). All formulations involve uncertain parameters that are fixed on specific case studies, or that can be adjusted in the tuning phase of a global model. In practice, it has been shown difficult to find such mixing formulations valid both for shallow and deep convection. Using high-resolution simulations, ~~(Del Genio and Wu 2010)~~ Del Genio and Wu (2010) show that entrainment rates best scale with $\frac{B}{w^2}$, B being the buoyancy, but that the scaling factor depends on convection depth. The distinction has also to be made between entrainment and dilution ~~(Hannah 2017)~~(Hannah 2017). For a given entrainment rate, the dilution of the updraft can indeed be reduced in the presence of moist shells as observed around convective clouds ~~(Heus and Jonker 2008 ; Glenn and Krueger 2014)~~(Heus and Jonker 2008 ; Glenn and Krueger 2014).

The lateral entrainment of environmental air into the updraft and the lateral detrainment of updraft air into the environment also control the vertical evolution of the mass-flux and fractional coverage of the updraft. The fractional detrainment rate~~is~~, also poorly constrained~~. In practice, it is~~, is either taken proportional to the fractional entrainment rate~~(Tiedtke 1989)~~, favored in a dry environment ~~(De Rooy and Siebesma 2008)~~ or where the updraft is negatively buoyant (around cloud top).

An other way to handle mixing processes in convective parameterizations is the episodic mixing and buoyancy sorting approach ~~(Raymond and Blyth 1986 ; Kain and Fritsch 1993 ; Emanuel 1991)~~(Raymond and Blyth 1986 ; Emanuel 1991 ; Kain and Fritsch 1993). In this approach, the ascending plume mixes at each level with environmental air at different rates, leading to a spectra of mixtures. After precipitation, ~~each mixture then goes up or~~ positively-buoyant mixtures entrain within the updraft while negatively-buoyant mixtures go down without additional mixing to ~~its~~ their level of neutral buoyancy where ~~it is detrained~~ they detrain into the environment. ~~Then the~~ The main difficulty is to specify the mixing rate spectrum at each level ~~(Grandpeix *et al.* 2004)~~(De Rooy *et al.* 2013).

Better understand and thus parameterize the control of convection by tropospheric humidity remains a key challenge to ensure to simulate accurate feedbacks between convection and its environment.

1.3.5 The role of water phase changes and rainfall

Water phase changes play a key role in convection dynamics by providing energy for parcels to gain buoyancy as explained above. They are also the source of convective rainfall which may in turn be partially reevaporated at lower levels – cooling and moistening the atmosphere – or reach the surface.

The simplest way of converting cloudy condensate to precipitation is to define a precipitation efficiency or autoconversion rate at each level, usually a function of pressure and updraft temperature ~~(Emanuel 1993)~~(Emanuel 1993). The partitioning between liquid and ice then depends on the temperature. More complex formulations rely on vertical velocity to specify particle size distributions and size-fall speed relationships to partition precipitation and detrainment (e.g. Del Genio *et al.* 2005). More complex microphysical schemes that calculate mass mixing ratio and number concentration of several hydrometeors (cloud liquid water, cloud ice, rain, snow, ...) exist that have been developed for cloud resolving models at kilometer-scale resolution. They are often used in LES but rarely in GCMs, even if such implementation exists ~~(Storer *et al.* 2015)~~ (Storer *et al.* 2015).

When precipitation falls outside cloudy air, it evaporates generating downdrafts. The impact of evaporatively-driven downdrafts can be taken into account in the same way than that of convective updrafts, by adding a contribution of convective downdrafts (subscript d) to the vertical transport:

$$\rho\overline{w'\phi'} = f_u \times (\underline{\Phi}\phi_u - \overline{\phi}) + f_d \times (\underline{\Phi}\phi_d - \overline{\phi}) \tag{1.25}$$

Additional hypotheses have then to be made to compute the downdrafts properties. Driven by the evaporation of precipitation, those downdrafts both cool (by evaporation of precipitation) and warm (by transporting dryer air from above the boundary-layer) the boundary-layer ~~(Betts 1976)~~ (Betts 1976). If the cooling effect is dominant, their impact is to stabilize the atmosphere and inhibit further convection. This is probably why those downdrafts are not always taken into account in parameterizations or implemented with a limited impact, because they can kill convection or make it intermittent in an unrealistic way. This can be overcome by adding some positive feedback between precipitation and convection via the role of cold pools.

1.3.6 The role of rainfall evaporation and cold pools

Observations back to the GATE campaign ~~(Zipser 1977)~~ (Zipser 1977) show that the evaporation of precipitation under convective systems leads to the formation of cold pools that spread at the surface as density currents. At the passage of the associated gust front, temperature drops of 2-10 K degrees, relative humidity and winds increase, with a feedback on turbulence and surface fluxes. By spreading close to the surface below the environmental air not yet affected by convection, cold pools result in a lifting which favors further convection at their border. This fundamental mechanism of the convection life cycle is a challenge to parameterize.

There have been some attempts to represent the re-inforcement of convection by cold pools without explicitly representing them, for example by adding some positive feedback of convective downdrafts on the updraft mass-flux ~~(Piriou *et al.* 2007)~~(Piriou *et al.* 2007), or by considering that entrainment depends on convective organization, diagnosed via the evaporation of precipition ~~(Mapes and Neale 2011)~~(Mapes and Neale 2011).

An attempt to represent explicitly the thermodynamical and dynamical effects of cold pools has been proposed by ~~(Grandpeix and Lafore 2010)~~Grandpeix and Lafore (2010). They consider a population of identical circular ~~wakes~~cold pools, of radius r and height h_{wk}, dispatched uniformly over an infinite plane containing the grid cell. The grid cell can again be decomposed into two different regions: the wake region, covered by cold pools, in which convective precipitation from the convection scheme falls, and the environment of ~~wakes~~ cold pools in which convective updrafts initiate. The parameterization introduces three new pronostic variables:
- the difference of temperature between the wake region (subscript wk) and its environment (subscript x): $\delta\theta_{wk} = \overline{\theta_{wk}} - \overline{\theta_x}$,
- the difference of specific humidity between the wake region and its environment: $\delta q_{wk} = \overline{q_{wk}} - \overline{q_x}$,
- the fractional area of the grid cell covered by ~~wakes σ_w and defined as:~~

$$\underline{\sigma_w = D_{wk}\pi r^2}$$

~~with D_{wk} the number of wakes by meter square (density)~~ cold pools σ_{wk}.
A vertical profile of the vertical velocity difference between the wake region and its environment

($\delta\omega$) is also introduced, which extends above the cold pool height, in order to take into account the existence of a mesoscale subsidence associated with the cold pool region as they spread at the surface.

~~They define~~ The expansion rate of the wake region is driven by the spreading speed ~~of the wake leading edge as~~C^* of the cold pool leading edge given by:

$$C^* = k^* \sqrt{2 \times WAPE} \tag{1.26}$$

$WAPE$ being the wake available potential energy defined as ~~$WAPE = -g \int_0^{h_w} \frac{\delta\theta_v}{\overline{\theta_v}} dz$~~ $WAPE = -g \int_0^{h_{wk}} \frac{\delta\theta_v}{\overline{\theta_v}} dz$ and k^* a tunable parameter.

~~Then, the expansion rate of the wakes is given by:~~

$$\partial_t \sigma_w = 2C^* \sqrt{\pi D_w} \sigma_w^{1/2}$$

In the approach proposed by ~~(Grandpeix and Lafore 2010)~~Grandpeix and Lafore (2010), cold pools affect convection in 2 ways:
- They ~~directly contribute to~~ modify the environment in which convection occur via their impact on Q_1 and Q_2,
- They provide a lifting energy in downwind of the gust front which is taken into account in the convective triggering and closure.

1.3.7 Accounting for meso-scale organization ?

The mass-flux approach used to parameterize convection assumes that the fraction of convective cells is small compared to the model grid size. This approach represent updrafts and downdrafts at the convective scale, that modify the environment, and provide information about cloud condensate and cover. The fact that convective cells can organize into a mesoscale cluster forming a large stratiform rain region and non-precipitating anvil is usually simply handled by a separate large-scale condensation scheme, i.e. a cloud scheme that computes cloud condensate and cover given the large-scale environmental profiles, with no associated subgrid vertical motions. Those clouds can last long after convective updrafts have vanished ~~(Roca *et al.* 2017)~~(Roca *et al.* 2017) . Observations have shown that mesoscale updrafts happen in the stratiform part of convective systems ~~(Houze Jr 2004)~~(Houze Jr 2004), driven by condensation heating and differential radiative heating between cloud base and cloud top ~~(Hartmann *et al.* 2018)~~(Hartmann *et al.* 2018). In addition, below the stratiform cloud, the evaporation of the stratiform rain cool and moisten the lower troposphere reinforcing a middle level inflow into the stratiform region ~~(Houze Jr 2004)~~ (Houze Jr 2004). There has been some attempts to parameterize mesoscale updrafts and downdrafts~~(Donner *et al.* 2011 ; Moncrieff *et al.* 2017)~~, but most GCM do not include any mesoscale circulations yet. The question is made even harder by the increase of resolution which makes this circulation partly subgrid scale and partly resolved when the resolution gets progressively down from 100km to 10km.

1.4 How to use parameterizations to understand scale interactions ?

We give here three illustrations of the use of parameterized convection to simulate and understand the role of scale interactions. The first two examples concern the scale interactions within the atmospheric column, between boundary layer turbulence, shallow convection and their large scale environment on one hand, and between shallow and deep convection and their environment on the other. The third example concerns the interaction between deep convection and the global atmospheric circulation.

Scale interactions will be illustrated based on simulations performed with the LMDZ general circulation model ~~(?)~~(Hourdin, Rio, Grandpeix, Madeleine, Cheruy, Rochetin, Jam, Musat, Idelkadi, Fairhead *et al.* 2020)

, the atmospheric component of the IPSL climate model ~~(Boucher *et al.* 2020)~~(Boucher *et al.* 2020) , which disposes of different sets of physical parameterizations that can be activated or not.

1.4.1 Interactions between turbulence and shallow convection and its impact on surface coupling

The scale interactions between small-scale turbulence, shallow convection and their environment is illustrated on Fig. 1.3 for a situation observed the 21st of June 1997 at the ARM SGP site in Oklahoma, known as the ARM cumulus test case of diurnal cycle of boundary layer convection ~~(Brown *et al.* 2002).~~ (Brown *et al.* 2002). Fig. 1.3a shows the vertical profile of potential temperature at initial time (dashed) and after 8 hours (thick pink curve) as simulated by the MESO-NH model ~~(?)~~ (Lac *et al.* 2018) in a LES mode. The initial profile is very stable, as classical at the end of the night. When the sun rises (here when the sensible heat flux increases), the lower part of the profile is destabilized with a negative vertical gradient of potential temperature close to the surface. Air parcels close to the surface get warmer in terms of potential temperature than the air above, so that an air parcel moved upward adiabatically gets warmer, thus lighter than the surrounding air. The parcel then rises until reaching a level with higher potential temperature. The rising parcels must be replaced by subsiding air. All those motions are made conserving potential temperature so that the potential temperature rapidly mixes between the surface and the inversion layer. Above the inversion, part of the air overshoots creating locally a cooling.

The LES is compared with the results of a simulation perfomed with a single column version of the LMDZ6A atmospheric model ~~(?)~~(Hourdin, Rio, Grandpeix, Madeleine, Cheruy, Rochetin, Jam, Musat, Idelkadi, Fair . Exactly the same forcing are applied in practice in both the LES and simulation with the Single Column Model (SCM). The diurnal cycle is forced by imposing a time evolution of the upward flux of heat and water (evaporation) at the surface.[2] In addition, imposed heating and moistening tendencies are added at each time step of the simulation, that represent the effect of dynamical advection of heat and moisture from the global circulation on the atmospheric column, which means that there is no feedback of convective processes on the large-scale circulation in this framework. In the SCM, the unresolved transport is represented by the combination of eddy diffusion (ED) – based on a prognostic equation of the turbulent kinetic energy ~~(Yamada 1983)~~ (Yamada 1983) –:

$$Q_1^{ED} = -\frac{1}{\rho}\frac{\partial}{\partial z}\left[-K_z \rho \frac{\partial \theta}{\partial z}\right] \tag{1.27}$$

and a mass flux (MF) parameterization of the organized structures of the convective boundary layer, the so-called "thermal plume model" ~~(Hourdin *et al.* 2002 ; Rio *et al.* 2010)~~(Hourdin *et al.* 2002 ; Rio *et al.* 2010) :

$$Q_1^{MF} = -\frac{1}{\rho}\frac{\partial}{\partial z}\left[f_u(\theta_u - \overline{\theta})\right] \tag{1.28}$$

The fact that the results of the LES are reasonably well reproduced by the SCM simulation (red and pink curves in panel a) using the "EDMF" approach, allows to understand the scale interactions between turbulent and convective motions that lead to this time evolution of the large scale potential temperature. Panel b shows the time integral of the various contributions to the time evolution of the potential temperature: large scale forcing, turbulent and convective transport, and phase change computed with a classical "large scale condensation" scheme ($Q_1^{LSC} = L_v(e-c)$). The red curve, the total evolution, is also the difference of the red and black curve of panel a.

The role of large scale condensation is weak for this fair-weather cumulus case. For this particular test case, the forcing is small as well. So most of the temperature evolution is explained by the sum of the contribution of the ED and MF parameterizations, which allows to better understand the respective role of turbulent diffusion and coherent structures in boundary-layer evolution. Close to the surface, the organized convection is not efficient enough to prevent unstable potential temperature profiles. In this part, called the surface layer, the upward heat transport is handled

[2] The forcing of this case is intentionally idealized to serve as a benchmark to parameterizations

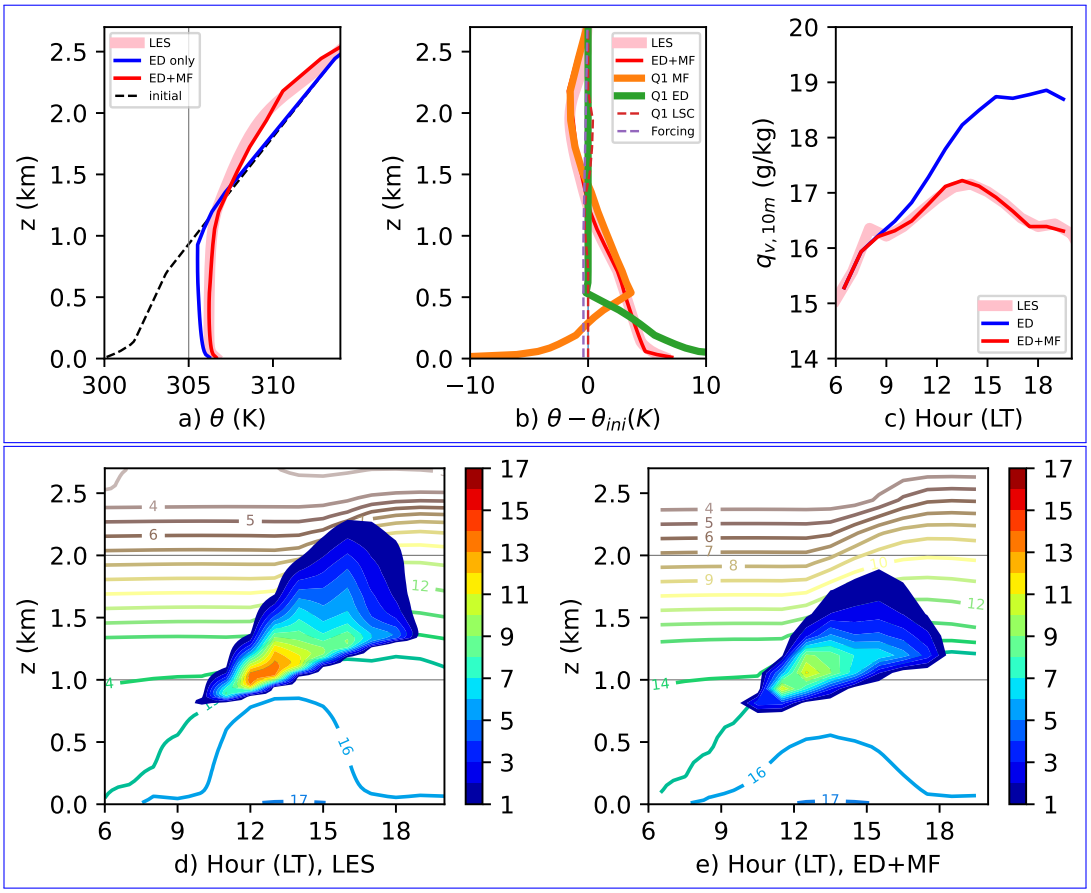

Figure 1.3: Shallow convection in a test case of diurnal cycle of cumulus clouds over continents (Arm cumulus case) as simulated in an LES (thick pink curves) with the MesoNH model and with the single column model (SCM) configuration of the global climate model LMDZ6A run with both eddy diffusion and mass-flux (ED+MF, red curves) or after deactivating the mass flux scheme (ED, blue curves). **a** : vertical profiles of potential temperature at initial time (dashed) and after 8 hours. **b** : The decomposition of the temperature change in the ED+MF simulation into contributions from ED and MF to Q1, forcing (imposed large scale advection and radiative heating), and effect of large scale condensation and evaporation. c) evolution of the near surface humidity (at 10m above surface in LMDZ and 12m in the LES). d) and e) : time evolution of the vertical profile for the specific humidity (contours, in g/kg) and cloud fraction (filled colors, in %) in the LES (e) and ED+MF standard version of LMDZ6A (right).

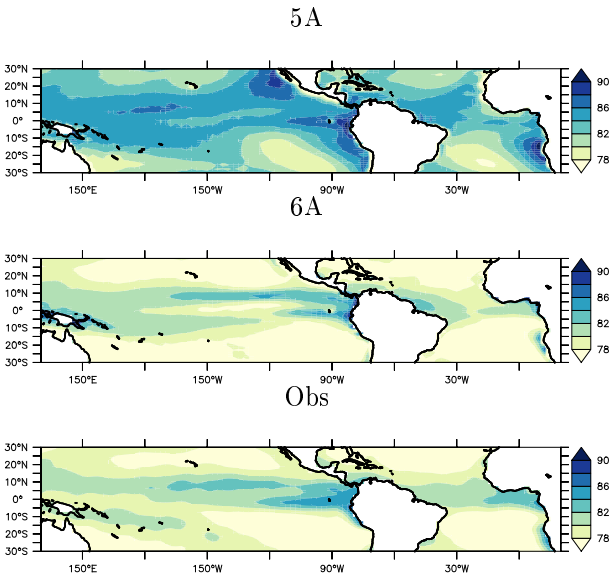

Figure 1.4: Annual mean near surface relative humidity (%) in ~~(da Silva *et al.* 1994)~~ da Silva *et al.* (1994) observations (top panel) and in forced by SST stand-alone atmospheric simulations. The mean bias, root-mean-square-error (RMSE) and correlation (CORR) with observations are shown at the top of each panel (same for the left and right columns).

by small scale unorganized convection. Higher up, the organized structures dominate the vertical transport, and control the rate of overshoot within the upper atmosphere ~~(Hourdin *et al.* 2019)~~ (Hourdin *et al.* 2019). There, the MF scheme stabilizes the atmosphere which in turn reduces the turbulent diffusion.

In order to understand the importance of shallow convection for climate, one can compare the above results with a simulation in which the MF component is deactivated. At first glance to Fig. 1.3a, such an ED simulation is capable of simulating the heating below inversion reasonably well, with a well mixed potential temperature. However, when looking in more details, the potential temperature profile below the inversion is slightly unstable everywhere (negative vertical gradient) while it is slightly stable in the upper part both in the LES and ED+MF simulations. This in fact is a direct consequence of the ED formulation which computes the vertical flux of potential temperature (or heat) with a sign opposite to the gradient (Eq. 1.27). Since the boundary layer is forced by the upward energy flux at the surface, the simulation has to wait until the potential temperature is unstable enough before being able to transport heat upward.

The compensation of the bad behavior of the local formulation by a slightly modified temperature gradient holds for temperature because of the coupling between diffusivity and temperature. Water on the opposite is a passive tracer for turbulent transport below clouds. The ED simulation is not efficient enough to transport the excess of air evaporated at the surface (imposed as a function of time in this simple test case) ; or to say it differently, the transport starts to be significant when enough water excess is accumulated close to the surface. The MF representation of the transport by organized convective plumes is at the opposite able to well represent the exchange between the surface humidity and the dry tropospheric air. This near-surface drying simulated on this specific case-study is obtained as well at global scale when introducing the MF parameterization in the LMDZ global circulation model, as illustrated in Fig. 1.4, giving a clear understanding of the way small scale turbulence and boundary layer convection control the near surface humidity.

The convective plumes of the boundary layer are also very important because they are at the origin of cumulus. Fig. 1.3f shows the cloud fraction diagnosed using the thermal plume properties to parameterize the shape and width of the subgrid-scale distribution of cloud water

following (Jam *et al.* 2013)Jam *et al.* (2013). The agreement with LES is qualitatively reasonable but shows a slight underestimation of the maximum cloud fraction and cloud vertical extension. Both the cloud fraction, via its impact on radiation, and the convective transport, via its impact on near-surface humidity and thus evaporation, are key drivers of the sea-surface temperature (Hourdin *et al.* 2015 ; Hourdin, Rio, Jam, Traore and Musat 2020)(Hourdin *et al.* 2015 ; Hourdin, Rio, Jam, Traore and . Mis-representing them lead to significant biases in sea surface temperature in global coupled ocean-atmosphere models.

1.4.2 Interactions between shallow and deep convection and its impact on the diurnal cycle of rainfall

The scale interactions between shallow and deep convection and the environment are illustrated considering a situation observed on the 27th of June 1997 at the same SGP ARM site. On this day, cumulus clouds first developed in the morning followed by the initiation of a thunderstorm with peaking rainfall in late afternoon. The so-called EUROCS case was defined from collected observations to evaluate the ability of models to simulate such a common situation (Guichard *et al.* 2004 ; Chaboureau *et al.* 2004)(Guichard *et al.* 2004). Here, to highlight the role of shallow convection in deep convection initiation, we put face to face two versions of the LMDZ model with different parameterizations for convection and clouds. In the LMDZ5A version (Hourdin *et al.* 2006)(Hourdin *et al.* 2006), the parameterization of boundary-layer turbulence is based on the diffusivity approach (Laval *et al.* 1981) a diffusivity approach with counter-gradient term and the convection scheme is based on (Emanuel 1991), which may handle either shallow or Emanuel (1991), which handle both shallow and deep convection. In the version LMDZ6A (?) (Hourdin, Rio, Grandpeix, Madeleine, Cheruy, Rochetin, Jam, Musat, Idelkadi, Fairhead *et al.* 2020) , a diffusive scheme is combined with the mass-flux scheme of boundary-layer thermals presented above, meant to represent dry and shallow convection. For deep convection, the (Emanuel 1991) Emanuel (1991) convection scheme is coupled with the parameterization of cold pools of (Grandpeix and Lafore 2010) Grandpeix and Lafore (2010) presented in section 10.3.6. The shallow and deep convection schemes are coupled together: the properties of the shallow convective updrafts are used to compute a lifting energy compared to the convective inhibition to trigger the deep convection scheme (Rochetin *et al.* 2014)(Rochetin *et al.* 2014), and to compute a lifting power used to derive the deep convective mass-flux at cloud base (Rio *et al.* 2009, 2013)(Rio *et al.* 2013). The simulated diurnal cycle of heating and moistening rates within the atmosphere the heating source Q_1 and moisture sink Q_2 as simulated by those two different versions of the LMDZ model are presented in Fig.1.5.

The impact of convection on its environment differs in the two versions, especially around midday. While deep convection bursts out quite early and peaks around midday in LMDZ5A, the version including an explicit representation of dry and cloudy boundary-layer thermals and cold pools rather simulate later and more long-lasting deep convection. This results in a different diurnal cycle of precipitation between the two models, precipitation peaking at 12:00LT and decreasing rapidly in LMDZ5A, while being triggered and maintained longer in LMDZ6A, leading to a peak at 15:00LT.

Fig.1.6 decomposes the total heat and moisture tendencies Q_1 and Q_2 simulated by LMDZ6A into the contributions of shallow convection, deep convection and cold pools, to better understand the interplay between each process. The contribution of shallow convection is computed using eq. 1.28 and is shown in the second line of Fig.1.6. As shown in the previous section on shallow convection, thermals initiating at the surface cool and dry the surface layer, warm and dry the mixed layer due to the compensating subsidence, and cool and moist the cloud layer in relation with cloud evaporation and water vapor detrainment.

Through its impact on the environment, shallow convection pre-conditions the occurence of deeper convection by progressively moistening the low troposphere via detrainment (Chaboureau *et al.* 2004) . This permits the formation of larger clouds that penetrate deeper into the troposphere. When parameterizations of shallow and deep convection are decoupled, this can be partly taken into account via the modification of large-scale profiles by shallow convection. It is also possible to ex-

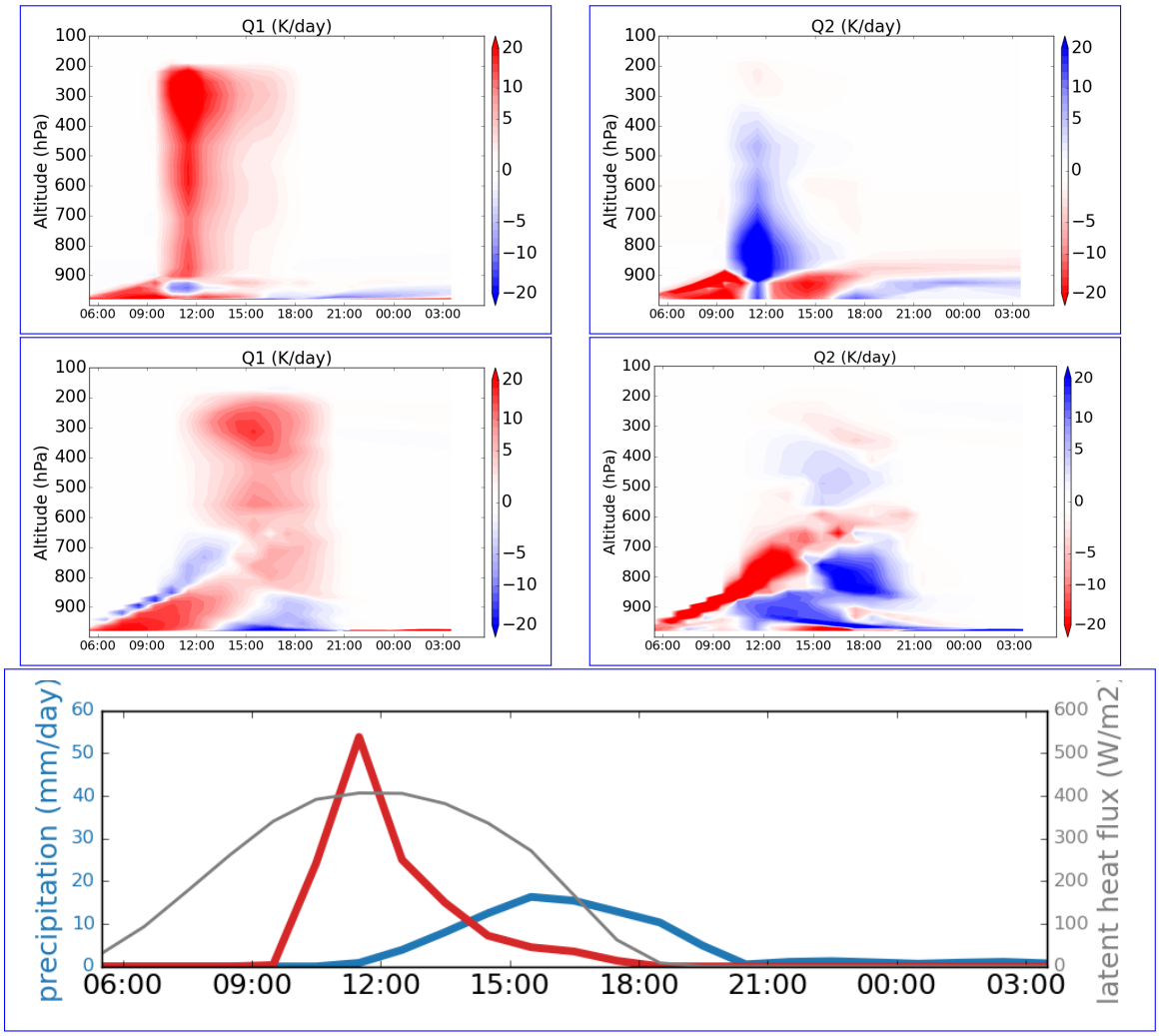

Figure 1.5: Time evolution of the vertical profile of the heating source Q_1 (K/day) and ~~moistening~~ the moisture sink Q_2 (~~g/kg~~K/day) ~~tendencies~~ as simulated in single-column mode by two different sets of parameterizations available in the LMDZ model on the EUROCS case: local diffusion and deep convection in LMDZ5A (top); and local diffusion, boundary-layer thermals, deep convection and cold pools in LMDZ6A (middle). The bottom panel shows the diurnal cycle of associated precipitation in LMDZ5A (red) and LMDZ6A (blue) and its phasing with the imposed surface latent heat flux (grey).~~ATTENTION: A FAIRE MONTRER Q2 ou DQ?~~

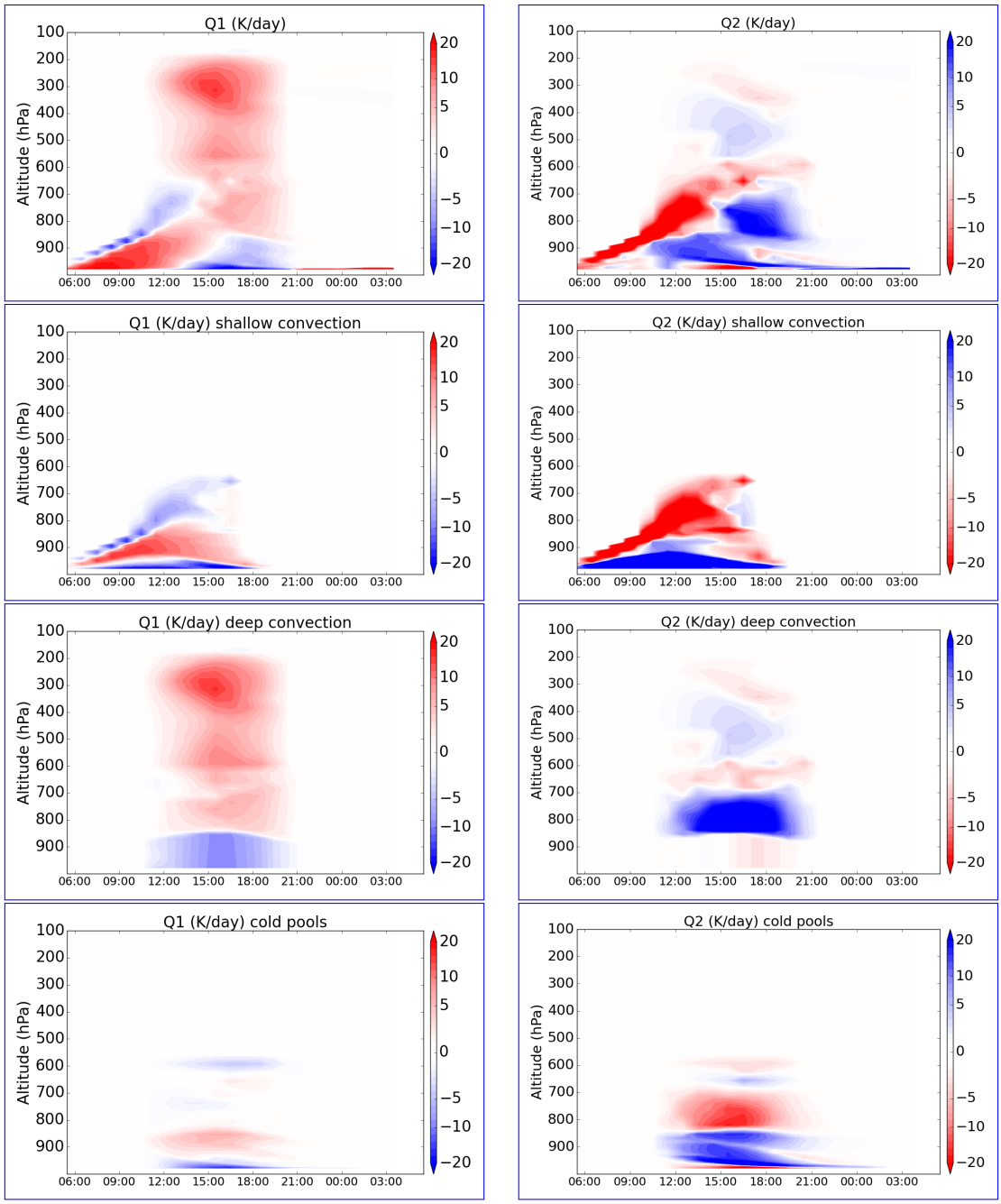

Figure 1.6: ~~Total Heating~~ Apparent heat source (top left, K/day) and ~~moistening~~ moisture sink (top right, ~~g/kg~~in K/day) ~~tendencies~~ as simulated by LMDZ6A on the EUROCS case decomposed into the contribution of the shallow convection scheme (second row), the deep convection scheme (third row) and the cold pool parameterization (last row).

plicitly couple the shallow and deep convective parameterizations to test hypothesis on how shallow convection acts to trigger deep convection. In the model used here for illustration, an estimation of the maximum vertical velocity within thermals and a probability that one boundary-layer thermal exceeds a given threshold are used to trigger the deep convection scheme ~~(Rochetin *et al.* 2014)~~ (Rochetin *et al.* 2014). Once the deep convection scheme initiated, the updraft and downdraft properties it simulates are used to compute its contribution to ~~heating rates~~ source terms following:

$$Q_1^{cv} = -\frac{1}{\rho}\frac{\partial}{\partial z}(f_u(\theta_u-\overline{\theta}) - \frac{1}{\rho}\frac{\partial}{\partial z}(f_d(\theta_d-\overline{\theta}) + L_v(c-e) \quad (1.29)$$

$$Q_2^{cv} = -L_v\frac{1}{\rho}\frac{\partial}{\partial z}(f_u(q_u-\overline{q}) - L_v\frac{1}{\rho}\frac{\partial}{\partial z}(f_d(q_d-\overline{q}) + L_v(c-e) \quad (1.30)$$

As shown in the third line of Fig. 1.6, the 27^{th} of June 1997 at the SGP ARM site, deep convection is initiated around midday. In the model, it heats and dry the mid-troposphere through the condensation and precipitation of water vapor. It also moistens the atmosphere at given levels, particularly at cloud top where cloud condensate is detrained into the environment. Below cloud base, it cools and moistens low levels via the evaporation of precipitation within unsaturated downdraft. The prominent impact of deep convection of warming and drying the troposphere is consistent with results from ~~(Yanai *et al.* 1973)~~ Yanai *et al.* (1973) who derived apparent heat source and moisture sink from temperature and moisture budgets derived from soundings around the Marshall Islands, and also with results from Cloud Resolving Models run on this specific case ~~(Guichard *et al.* 2004)~~(Guichard *et al.* 2004).

In the model used here for illustration, the cold pool parameterization also contributes to Q1 and Q2 via:

$$Q_1^{wk} = C_p(\partial_t\sigma_{\underline{w}wk} - e_{\underline{w}wk})\delta\theta_{wk} - C_p\sigma_{\underline{w}wk}(1-\sigma_{\underline{w}wk})\delta\omega\partial_p\delta\theta_{wk} \quad (1.31)$$

$$Q_2^{wk} = \frac{C_p}{L_v}(\partial_t\sigma_{\underline{w}wk} - e_{\underline{w}wk})\delta q_{\underline{v}wk} - \frac{C_p}{L_v}\sigma_{\underline{w}wk}(1-\sigma_{\underline{w}wk})\delta\omega\partial_p\delta q_{\underline{v}wk} \quad (1.32)$$

The first right hand side term takes into account the impact of cold pool spreading and entrainment of environmental air inside cold pools while the second right hand side term represents the effect of differential vertical advection between the cold pool region and its environment. ~~The direct thermodynamical effect of cold pools is quite weak with a slight cooling of the environment~~ Cold pools cool and moist close to the surface as they spread at the surface. Above~~the cold pool height, the atmosphere is warmed instead via the effect of entrainment of dry air within~~ , their effect is rather driven by the differential vertical advection between the cold pool ~~subsiding region . Regarding moisture,~~ region and its environment, namely the combination of a drying and warming induced by a mesoscale subsidence within the cold pool region and a moistening and warming due to the ~~effect of cold pool is to moist close to the surface as a consequence of rain evaporation. The effect of differential vertical advection in the wake and environmental regions leads to dry the mixed layer and moist the low troposphere above (ici checker avec Jean-Yves). More importantly, cold pools also~~ compensatory ascendance in its environment. In the model the dynamical effect of cold pools on convection is also taken into account as they provide a lifting energy at their border that can trigger new deep convective cells and a lifting power that contributes to deep convective intensity. This ~~effect is taken into account in LMDZ6A (Rio *et al.* 2013), which~~ explains why deep convection is maintained longer ~~than~~ in the simulation ~~without cold pool representation~~ 6A compared to simulation 5A in which the evaporation of convective precipitation rapidly inhibates further convection.

This shift of the timing of maximum of precipitation over land simulated here on a single case-study holds for the entire continental regions as illustrated in Fig. 1.7 comparing LMDZ5A and LMDZ6A simulations with TRMM observations. The ~~timing of continental rainfall in turn may have direct implication for the radiative impact of associated clouds. The~~ fact that most convective

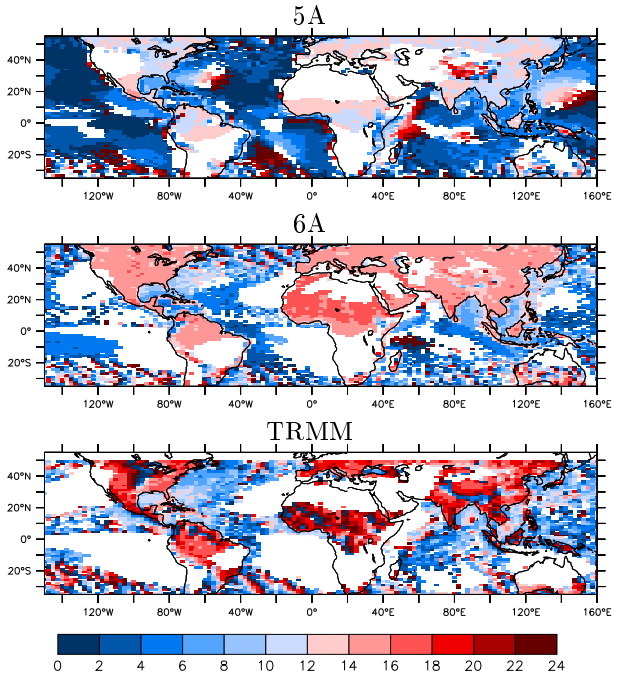

Figure 1.7: Time in the day of maximum rainfall computed as the phase of the first harmonic of the mean diurnal cycle for June-July-August as simulated in LMDZ5A (top), LMDZ6A (middle) and observed by TRMM (bottom).

parameterizations simulate continental rainfall peaking around midday instead of late-afternoon has been for long seen as a deadlock of convective parameterizations ~~(Randall *et al.* 2003)~~(Randall *et al.* 2003) . This example illustrates that it is not only possible to simulate a realistic diurnal cycle with a set of physical parameterizations, but that the physical parameterizations also enable us to understand the interactions between the different processes leading to the observed diurnal cycle.

1.4.3 Interactions between convection and the large-scale circulation and its impact on Hadley cells

In this last section, we illustrate how the GCM framework can be used to simulate and understand the interactions between convection and the large-scale circulation. For illustration purpose, we reduce the complexity of the atmospheric flow and focus on the Hadley circulation, relying on idealized global simulations in aqua-planet mode. In this framework, the whole planet surface is covered by ocean and the model is forced by a prescribed zonally symetric SST with a maximum of 27^oC at the equator ~~(ref)~~ (Queslati and Bellon 2013) and a perpetual equinoctial solar insolation including the diurnal cycle~~(A VERIFIER)~~.

The first panel of Fig. 1.8 shows the zonal average of the annual mean of the stream function Ψ (kg/s) associated with the zonally averaged mean meridional circulation as simulated by LMDZ6A. The ascending branchs are located at the equator and the subsiding branchs around 20S and 20N. The heating tendencies associated with this dynamical circulation are shown in color. The dynamical flow cools the whole atmospheric column between approximately 12.5S and 12.5N in the ascending branch of the Hadley circulation. In the subsiding branchs, it heats the atmosphere above 900hPa, the boundary-layer height, and cools it below. The left panels of Fig. 1.8 show the heating rate associated with sub-grid physical processes. As the tendencies and circulations are symmetrical about the equator, each component of the total heating rate is shown for one hemisphere of the aquaplanet. One can note that on annual mean, the total tendency associated with physical processes and the one associated with the dynamical circulation balance each other.

It is the case as well in a full GCM since the temperature and humidity changes are bounded so that the averaged tendencies decrease with the time intervall considered (A CLARIFIER). The physical heating rate is further decomposed into the vertical transport (turbulence, shallow and deep convection), the radiation and the large-scale condensation scheme contributions. The major contributor to the physical heating rate comes from the vertical transport by turbulence and convection. Consistently with results obtained previously on specific case-studies, deep convection heats the troposphere (on either side of the equator), while shallow convection heats the boundary layer and cools the mid-troposphere (beyond 15^oC). Large-scale condensation heats inside clouds and cools below by the evaporation of precipitation. The overall impact of radiation is to cool the atmosphere, with a maximum cooling at the location of shallow clouds.

The right panels of Fig. 1.8 show the same tendencies simulated by LMDZ5A, meaning with a different representation of convection and clouds. The strength of the simulated circulation is slightly weaker and the width of the ascending branch slightly narrower. Main differences arise from the vertical profile of the convective heating rate in the ascending region and the height and strength of radiative cooling in the subsidence region. In this particular case, the circulation is stronger in LMDZ6A in relation with less heating at mid-levels in the ascending region, due to the cooling impact of shallow convection that reduces the heating rate from deep convection and a stronger cooling at the same levels in the subsiding region, in relation with more shallow convective clouds located higher.

The zonal average of precipitation is shown in the top panel of Fig. 1.9. The stronger and wider ascending branch of the Hadley circulation is associated with a stronger and wider intertropical convergence zone in LMDZ6A compared with LMDZ5A. The excess of precipitation in LMDZ6A can be explained by more evaporation at the surface (dashed lines), which can be attributed to the representation of boundary-layer thermals which dry the surface and enhances evaporation, as shown in section 4.1 (Fig. 1.9, bottom panel).

Note that LMDZ5A and LMDZ6A not only differ by their physical parameterization package but also by their value of internal parameters that have been calibrated to ensure, among others targets, energy balance at the top of the atmosphere. Disentangling the respective role of physical formulations versus parameter values in the two model behavior differences is another challenge that requires additional sensitivity experiments and that will be made easier by the use of automatic tools to explore the possible ranges of parameters.

This comparison between two versions of a model with different ways of representing physical processes illustrate how parameterizations embedded in GCM can be used to simulate and understand scale interactions in the atmosphere, by giving the opportunity to add or suppress a specific process, test hypothesis, and simulate climates that may never be observed.

1.5 Conclusion

Since the pioneer times, GCMs have proven their ability to anticipate the weather of the next few days; they have also predicted in the late 70s the global warming which was not observed at that time ~~(?Manabe *et al.* 1965)~~(?Manabe *et al.* 1965). The success of these models in prediction may have partly obscured the extent to which they constitute a particularly powerful framework for studying and understanding scale interactions in the atmosphere. As Arakawa himself, a pioneer of parmeterization development, wrote in 2004 : *"It should be emphasized here that the need for parameterizations is not limited to "numerical" models. Formulating the statistical behavior of small-scale processes is needed for understanding large-scale phenomena regardless of weather we use numerical, theoretical, or conceptual models. Even under a hypothetical situation in which we have a model that resolves all scales, it alone does not automatically give us an understanding of scale interactions. Understanding inevitably requires simplifications, including various levels of "parameterizations," either explicitly or implicitly, which are quantitative statements on the statistical behavior of the processes involved. Parameterizations thus have their own scientific merits."*

Proposing a new parameterization, implementing it in a global model, and assessing the effect

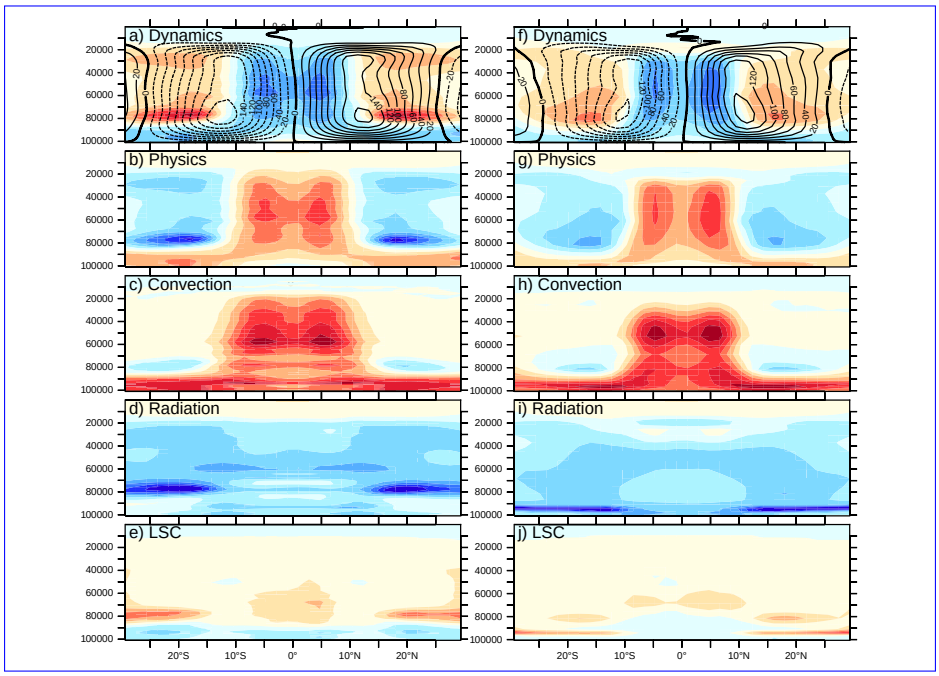

Figure 1.8: Decomposition of the different contributions to the zonally-averaged annual heating rate in aqua-planet simulations performed with LMDZ6A (left) and LMDZ5A (right). The dynamical tendency is shown on the first row, together with the current function ~~*Psi*~~ Ψ (kg/s) associated with the Hadley circulation. The positive values as solid black line correspond to a clockwise circulation, while the negative values in dashed lines corresponds to a counter clockwise circulation. The second and third rows display the total physical tendency and its decomposition into vertical sub-grid transport, radiation and large-scale condensation.

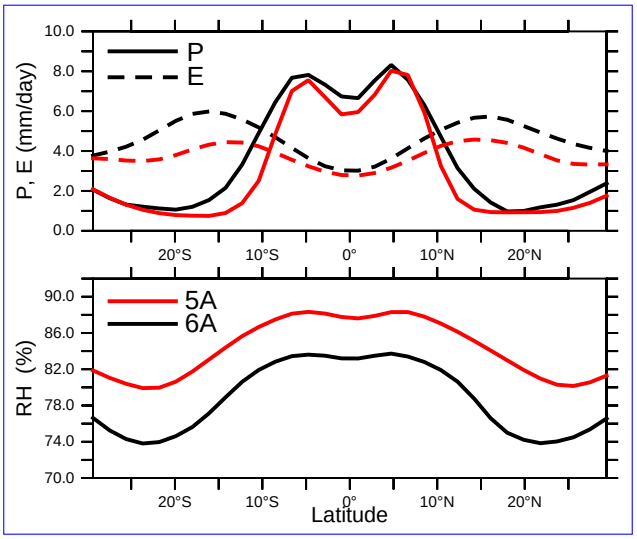

Figure 1.9: Zonal average of annual mean precipitation (solid), evaporation (dashed) and relative humidity at 2m as simulated by LMDZ6A (red) and LMDZ5A (black) in aqua-planet simulations.

on the simulated circulation and climate is driving the work of parameterization development. The fact that involved parameters have to be retuned after a change of parameterization to ensure global energy balance at the top of the atmosphere has long be seen as an obstacle to understand how sub-grid processes affect the large-scale. The recent development of approaches of machine assisted calibration of the free parameters is a major change in the development of parameterizations, since it will help understand the respective role of physical formulations versus parameter calibration in the model emergent simulated properties.

The next frontier GCMs have to overcome is the representation of deep convection organized at the mesoscale, as several theoretical studies have shown the importance of a good representation of heating rates associated to the stratiform part of convective systems to accurately represent the observed modes of variability such as the Madden-Julian Oscillation and the wave spectra ~~(Lappen and Schumacher 2012 ; Chen *et al.* 2021). If a part of the community turns~~ (Lappen and Schumacher 2012 ; Chen *et al.* 2021). If an option to tackle this issue can be to turn to resolution at the kilometer-scale or machine learning techniques trained on large-eddy simulations~~to tackle this issue~~, developping parameterization of mesoscale circulations within organized convective systems remains an unmissable path to ensure main drivers of the life cycle of convective systems are understood~~and~~ , and to study further the interactions between mesoscale convective systems and the large-scale circulation within the atmosphere.

key points / take-home messages

- The general circulation model framework, which separates the resolved large-scale flow from sub-grid physical processes, is an essential tool to simulate and understand scale interactions in the atmosphere.
- Convection parameterizations are based on a simplified representation of the main physical processes, including vertical transport, mixing and microphysics. Current challenge is to enable models to correctly represent the impact of the mesoscale organization of convective systems on their environment.
- Shallow and deep convective processes have an impact on surface fluxes, large-scale circulation and precipitation distribution and variability and therefore play a key role in weather and climate.

Chapter 2

Bibliography

Abdella, K., McFarlane, N. (1997), A new second-order turbulence closure scheme for the planetary boundary layer, *Journal of the atmospheric sciences*, 54(14), 1850–1867.

Arakawa, A. (2004), The cumulus parameterization problem: Past, present, and future, *Journal of Climate*, 17(13), 2493–2525.

Arakawa, A., Schubert, W. H. (1974), Interaction of a cumulus cloud ensemble with the large-scale environment, part i, *Journal of the atmospheric sciences*, 31(3), 674–701.

Bechtold, P., Köhler, M., Jung, T., Doblas-Reyes, F., Leutbecher, M., Rodwell, M. J., Vitart, F., Balsamo, G. (2008), Advances in simulating atmospheric variability with the ecmwf model: From synoptic to decadal time-scales, *Quarterly Journal of the Royal Meteorological Society: A journal of the atmospheric sciences, applied meteorology and physical oceanography*, 134(634), 1337–1351.

Betts, A. K. (1976), The thermodynamic transformation of the tropical subcloud layer by precipitation and downdrafts, *Journal of atmospheric sciences*, 33(6), 1008–1020.

Bogenschutz, P., Gettelman, A., Morrison, H., Larson, V., Schanen, D., Meyer, N., Craig, C. (2012), Unified parameterization of the planetary boundary layer and shallow convection with a higher-order turbulence closure in the community atmosphere model: Single-column experiments, *Geoscientific Model Development*, 5(6), 1407–1423.

Boucher, O., Servonnat, J., Albright, A. L., Aumont, O., Balkanski, Y., Bastrikov, V., Bekki, S., Bonnet, R., Bony, S., Bopp, L. *et al.* (2020), Presentation and evaluation of the ipsl-cm6a-lr climate model, *Journal of Advances in Modeling Earth Systems*, 12(7), e2019MS002010.

Bougeault, P. (1985), A simple parameterization of the large-scale effects of cumulus convection, *Monthly Weather Review*, 113(12), 2108–2121.

Bretherton, C. S., Park, S. (2009), A new moist turbulence parameterization in the community atmosphere model, *Journal of Climate*, 22(12), 3422–3448.

Brown, A., Cederwall, R. T., Chlond, A., Duynkerke, P. G., Golaz, J.-C., Khairoutdinov, M., Lewellen, D., Lock, A., MacVean, M., Moeng, C.-H. *et al.* (2002), Large-eddy simulation of the diurnal cycle of shallow cumulus convection over land, *Quarterly Journal of the Royal Meteorological Society: A journal of the atmospheric sciences, applied meteorology and physical oceanography*, 128(582), 1075–1093.

Chaboureau, J.-P., Guichard, F., Redelsperger, J.-L., Lafore, J.-P. (2004), The role of stability and moisture in the diurnal cycle of convection over land, *Quarterly Journal of the Royal Meteorological Society: A journal of the atmospheric sciences, applied meteorology and physical oceanography*, 130(604), 3105–3117.

Chatfield, R. B., Brost, R. A. (1987), A two-stream model of the vertical transport of trace species in the convective boundary layer, *Journal of Geophysical Research: Atmospheres*, 92(D11), 13263–13276.

Chen, C.-C., Richter, J., Liu, C., Moncrieff, M., Tang, Q., Lin, W., Xie, S., Rasch, P. J. (2021), Effects of organized convection parameterization on the mjo and precipitation in e3smv1. part i: Mesoscale heating, *Journal of Advances in Modeling Earth Systems*, 13(6), e2020MS002401.

Couvreux, F., Hourdin, F., Williamson, D., Roehrig, R., Volodina, V., Villefranque, N., Rio, C., Audouin, O., Salter, J., Bazile, E. *et al.* (2021), Process-based climate model development harnessing machine learning: I. a calibration tool for parameterization improvement, *Journal of Advances in Modeling Earth Systems*, 13(3), e2020MS002217.

da Silva, A. M., Young, C. C., Levitus, S. (1994), Atlas of surface marine data 1994, volume 1: algorithms and procedures, , .

De Rooy, W. C., Bechtold, P., Fröhlich, K., Hohenegger, C., Jonker, H., Mironov, D., Pier Siebesma, A., Teixeira, J., Yano, J.-I. (2013), Entrainment and detrainment in cumulus convection: An overview, *Quarterly Journal of the Royal Meteorological Society*, 139(670), 1–19.

De Rooy, W. C., Siebesma, A. P. (2008), A simple parameterization for detrainment in shallow cumulus, *Monthly weather review*, 136(2), 560–576.

Deardorff, J. (1966), The counter-gradient heat flux in the lower atmosphere and in the laboratory, *Journal of the Atmospheric Sciences*, 23(5), 503–506.

Deardorff, J. W. *et al.* (1970), Convective velocity and temperature scales for the unstable planetary boundary layer and for rayleigh convection, *J. atmos. Sci*, 27(8), 1211–1213.

Del Genio, A. D., Kovari, W., Yao, M.-S., Jonas, J. (2005), Cumulus microphysics and climate sensitivity, *Journal of climate*, 18(13), 2376–2387.

Del Genio, A. D., Wu, J. (2010), The role of entrainment in the diurnal cycle of continental convection, *Journal of Climate*, 23(10), 2722–2738.

Del Genio, A., Yao, M. (1993), *Efficient Cumulus Parameterization for Long-Term Climate Studies: The GISS Scheme*, pp. 181–184.

Derbyshire, S., Beau, I., Bechtold, P., Grandpeix, J.-Y., Piriou, J.-M., Redelsperger, J.-L., Soares, P. (2004), Sensitivity of moist convection to environmental humidity, *Quarterly Journal of the Royal Meteorological Society: A journal of the atmospheric sciences, applied meteorology and physical oceanography*, 130(604), 3055–3079.

Donner, L. J., Wyman, B. L., Hemler, R. S., Horowitz, L. W., Ming, Y., Zhao, M., Golaz, J.-C., Ginoux, P., Lin, S.-J., Schwarzkopf, M. D. *et al.* (2011), The dynamical core, physical parameterizations, and basic simulation characteristics of the atmospheric component am3 of the gfdl global coupled model cm3, *Journal of Climate*, 24(13), 3484–3519.

Emanuel, K. A. (1991), A scheme for representing cumulus convection in large-scale models, *Journal of the atmospheric sciences*, 48(21), 2313–2329.

Emanuel, K. A. (1993), A cumulus representation based on the episodic mixing model: the importance of mixing and microphysics in predicting humidity, *in* The representation of cumulus convection in numerical models, Springer, pp. 185–192.

Glenn, I. B., Krueger, S. K. (2014), Downdrafts in the near cloud environment of deep convective updrafts, *Journal of Advances in Modeling Earth Systems*, 6(1), 1–8.

Grandpeix, J.-Y., Lafore, J.-P. (2010), A density current parameterization coupled with emanuel's convection scheme. part i: The models, *Journal of the Atmospheric Sciences*, 67(4), 881–897.

Grandpeix, J.-Y., Phillips, V., Tailleux, R. (2004), Improved mixing representation in emanuel's convection scheme, *Quarterly Journal of the Royal Meteorological Society: A journal of the atmospheric sciences, applied meteorology and physical oceanography*, 130(604), 3207–3222.

Gregory, D. (2001), Estimation of entrainment rate in simple models of convective clouds, *Quarterly Journal of the Royal Meteorological Society*, 127(571), 53–72.

Guichard, F., Petch, J., Redelsperger, J.-L., Bechtold, P., Chaboureau, J.-P., Cheinet, S., Grabowski, W., Grenier, H., Jones, C., Köhler, M. *et al.* (2004), Modelling the diurnal cycle of deep precipitating convection over land with cloud-resolving models and single-column

models, *Quarterly Journal of the Royal Meteorological Society: A journal of the atmospheric sciences, applied meteorology and physical oceanography*, 130(604), 3139–3172.

Hannah, W. M. (2017), Entrainment versus dilution in tropical deep convection, *Journal of the Atmospheric Sciences*, 74(11), 3725–3747.

Hartmann, D. L., Gasparini, B., Berry, S. E., Blossey, P. N. (2018), The life cycle and net radiative effect of tropical anvil clouds, *Journal of Advances in Modeling Earth Systems*, 10(12), 3012–3029.

Harvey, N. J., Daleu, C. L., Stratton, R. A., Plant, R. S., Woolnough, S. J., Stirling, A. J. (2022), The impact of surface heterogeneity on the diurnal cycle of deep convection, *Quarterly Journal of the Royal Meteorological Society*, 148(749), 3509–3527.

Heus, T., Jonker, H. J. (2008), Subsiding shells around shallow cumulus clouds, *Journal of the Atmospheric Sciences*, 65(3), 1003–1018.

Holtslag, A., Boville, B. (1993), Local versus nonlocal boundary-layer diffusion in a global climate model, *Journal of climate*, 6(10), 1825–1842.

Hourdin, F., Couvreux, F., Menut, L. (2002), Parameterization of the dry convective boundary layer based on a mass flux representation of thermals, *Journal of the atmospheric sciences*, 59(6), 1105–1123.

Hourdin, F., Găinusă-Bogdan, A., Braconnot, P., Dufresne, J.-L., Traore, A.-K., Rio, C. (2015), Air moisture control on ocean surface temperature, hidden key to the warm bias enigma, *Geophysical Research Letters*, 42(24), 10–885.

Hourdin, F., Jam, A., Rio, C., Couvreux, F., Sandu, I., Lefebvre, M.-P., Brient, F., Idelkadi, A. (2019), Unified parameterization of convective boundary layer transport and clouds with the thermal plume model, *Journal of Advances in Modeling Earth Systems*, 11(9), 2910–2933.

Hourdin, F., Mauritsen, T., Gettelman, A., Golaz, J.-C., Balaji, V., Duan, Q., Folini, D., Ji, D., Klocke, D., Qian, Y. *et al.* (2017), The art and science of climate model tuning, *Bulletin of the American Meteorological Society*, 98(3), 589–602.

Hourdin, F., Musat, I., Bony, S., Braconnot, P., Codron, F., Dufresne, J.-L., Fairhead, L., Filiberti, M.-A., Friedlingstein, P., Grandpeix, J.-Y. *et al.* (2006), The lmdz4 general circulation model: climate performance and sensitivity to parametrized physics with emphasis on tropical convection, *Climate Dynamics*, 27, 787–813.

Hourdin, F., Rio, C., Grandpeix, J.-Y., Madeleine, J.-B., Cheruy, F., Rochetin, N., Jam, A., Musat, I., Idelkadi, A., Fairhead, L. *et al.* (2020), Lmdz6a: The atmospheric component of the ipsl climate model with improved and better tuned physics, *Journal of Advances in Modeling Earth Systems*, 12(7), e2019MS001892.

Hourdin, F., Rio, C., Jam, A., Traore, A.-K., Musat, I. (2020), Convective boundary layer control of the sea surface temperature in the tropics, *Journal of Advances in Modeling Earth Systems*, 12(6), e2019MS001988.

Hourdin, F., Williamson, D., Rio, C., Couvreux, F., Roehrig, R., Villefranque, N., Musat, I., Fairhead, L., Diallo, F. B., Volodina, V. (2021), Process-based climate model development harnessing machine learning: Ii. model calibration from single column to global, *Journal of Advances in Modeling Earth Systems*, 13(6), e2020MS002225.

Houze Jr, R. A. (2004), Mesoscale convective systems, *Reviews of Geophysics*, 42(4).

Jam, A., Hourdin, F., Rio, C., Couvreux, F. (2013), Resolved versus parametrized boundary-layer plumes. part iii: Derivation of a statistical scheme for cumulus clouds, *Boundary-layer meteorology*, 147(3), 421–441.

Kain, J. S., Fritsch, J. M. (1993), Convective parameterization for mesoscale models: The kain-fritsch scheme, *in* The representation of cumulus convection in numerical models, Springer, pp. 165–170.

Khairoutdinov, M., Randall, D. (2006), High-resolution simulation of shallow-to-deep convection

transition over land, *Journal of the atmospheric sciences*, 63(12), 3421–3436.

Kuo, H.-L. (1965), On formation and intensification of tropical cyclones through latent heat release by cumulus convection, *Journal of the atmospheric sciences*, 22(1), 40–63.

Lac, C., Chaboureau, J.-P., Masson, V., Pinty, J.-P., Tulet, P., Escobar, J., Leriche, M., Barthe, C., Aouizerats, B., Augros, C. *et al.* (2018), Overview of the meso-nh model version 5.4 and its applications, *Geoscientific Model Development*, 11(5), 1929–1969.

Lappen, C.-L., Randall, D. A. (2001), Toward a unified parameterization of the boundary layer and moist convection. part i: A new type of mass-flux model, *Journal of the Atmospheric Sciences*, 58(15), 2021–2036.

Lappen, C.-L., Schumacher, C. (2012), Heating in the tropical atmosphere: what level of detail is critical for accurate mjo simulations in gcms?, *Climate dynamics*, 39, 2547–2568.

Larson, V. E., Golaz, J.-C. (2005), Using probability density functions to derive consistent closure relationships among higher-order moments, *Monthly Weather Review*, 133(4), 1023–1042.

Laval, K., Sadourny, R., Serafini, Y. (1981), Land surface processes in a simplified general circulation model, *Geophysical & Astrophysical Fluid Dynamics*, 17(1), 129–150.

LeMone, M. A., Pennell, W. T. (1976), The relationship of trade wind cumulus distribution to subcloud layer fluxes and structure, *Monthly Weather Review*, 104(5), 524–539.

Manabe, S., Smagorinsky, J., Strickler, R. F. (1965), Simulated climatology of a general circulation model with a hydrologic cycle, *Monthly Weather Review*, 93(12), 769–798.

Mapes, B., Neale, R. (2011), Parameterizing convective organization to escape the entrainment dilemma, *Journal of Advances in Modeling Earth Systems*, 3(2).

Moncrieff, M. W., Liu, C., Bogenschutz, P. (2017), Simulation, modeling, and dynamically based parameterization of organized tropical convection for global climate models, *Journal of the Atmospheric Sciences*, 74(5), 1363–1380.

Neggers, R., Siebesma, A., Jonker, H. (2002), A multiparcel model for shallow cumulus convection, *Journal of the Atmospheric Sciences*, 59(10), 1655–1668.

Ooyama, K. (1964), A dynamical model for the study of tropical cyclone development., *Geofisica Internacional (Mexico)*, 4, 187–198.

Oueslati, B., Bellon, G. (2013), Tropical precipitation regimes and mechanisms of regime transitions: Contrasting two aquaplanet general circulation models, *Climate dynamics*, 40, 2345–2358.

Park, S. (2014), A unified convection scheme (unicon). part i: Formulation, *Journal of the Atmospheric Sciences*, 71(11), 3902–3930.

Pergaud, J., Masson, V., Malardel, S., Couvreux, F. (2009), A parameterization of dry thermals and shallow cumuli for mesoscale numerical weather prediction, *Boundary-layer meteorology*, 132, 83–106.

Piriou, J.-M., Redelsperger, J.-L., Geleyn, J.-F., Lafore, J.-P., Guichard, F. (2007), An approach for convective parameterization with memory: Separating microphysics and transport in grid-scale equations, *Journal of the Atmospheric Sciences*, 64(11), 4127–4139.

Pleim, J. E., Xiu, A. (1995), Development and testing of a surface flux and planetary boundary layer model for application in mesoscale models, *Journal of Applied Meteorology (1988-2005)*, pp. 16–32.

Randall, D., Khairoutdinov, M., Arakawa, A., Grabowski, W. (2003), Breaking the cloud parameterization deadlock, *Bulletin of the American Meteorological Society*, 84(11), 1547–1564.

Raymond, D. J. (1994), Convective processes and tropical atmospheric circulations, *Quarterly Journal of the Royal Meteorological Society*, 120(520), 1431–1455.
URL: *https://rmets.onlinelibrary.wiley.com/doi/abs/10.1002/qj.49712052002*

Raymond, D. J., Blyth, A. M. (1986), A stochastic mixing model for nonprecipitating cumulus clouds, *Journal of Atmospheric Sciences*, 43(22), 2708–2718.

Rio, C., Del Genio, A. D., Hourdin, F. (2019), Ongoing breakthroughs in convective parameterization, *Current Climate Change Reports*, 5, 95–111.

Rio, C., Grandpeix, J.-Y., Hourdin, F., Guichard, F., Couvreux, F., Lafore, J.-P., Fridlind, A., Mrowiec, A., Roehrig, R., Rochetin, N. *et al.* (2013), Control of deep convection by sub-cloud lifting processes: the alp closure in the lmdz5b general circulation model, *Climate dynamics*, 40, 2271–2292.

Rio, C., Hourdin, F. (2008), A thermal plume model for the convective boundary layer: Representation of cumulus clouds, *Journal of the atmospheric sciences*, 65(2), 407–425.

Rio, C., Hourdin, F., Couvreux, F., Jam, A. (2010), Resolved versus parametrized boundary-layer plumes. part ii: continuous formulations of mixing rates for mass-flux schemes, *Boundary-layer meteorology*, 135, 469–483.

Rio, C., Hourdin, F., Grandpeix, J.-Y., Lafore, J.-P. (2009), Shifting the diurnal cycle of parameterized deep convection over land, *Geophysical Research Letters*, 36(7).

Roca, R., Fiolleau, T., Bouniol, D. (2017), A simple model of the life cycle of mesoscale convective systems cloud shield in the tropics, *Journal of Climate*, 30(11), 4283–4298.

Rochetin, N., Couvreux, F., Grandpeix, J.-Y., Rio, C. (2014), Deep convection triggering by boundary layer thermals. part i: Les analysis and stochastic triggering formulation, *Journal of the Atmospheric Sciences*, 71(2), 496–514.

Rochetin, N., Couvreux, F., Guichard, F. (2017), Morphology of breeze circulations induced by surface flux heterogeneities and their impact on convection initiation, *Quarterly Journal of the Royal Meteorological Society*, 143(702), 463–478.

Siebesma, A., Cuijpers, J. (1995), Evaluation of parametric assumptions for shallow cumulus convection, *Journal of Atmospheric Sciences*, 52(6), 650–666.

Siebesma, A. P., Soares, P. M., Teixeira, J. (2007), A combined eddy-diffusivity mass-flux approach for the convective boundary layer, *Journal of the atmospheric sciences*, 64(4), 1230–1248.

Simpson, J., Wiggert, V. (1969), Models of precipitating cumulus towers, *Monthly Weather Review*, 97(7), 471–489.

Soares, P., Miranda, P., Siebesma, A., Teixeira, J. (2004), An eddy-diffusivity/mass-flux parametrization for dry and shallow cumulus convection, *Quarterly Journal of the Royal Meteorological Society: A journal of the atmospheric sciences, applied meteorology and physical oceanography*, 130(604), 3365–3383.

Storer, R. L., Zhang, G. J., Song, X. (2015), Effects of convective microphysics parameterization on large-scale cloud hydrological cycle and radiative budget in tropical and midlatitude convective regions, *Journal of Climate*, 28(23), 9277–9297.

Stull, R. B. (1984), Transilient turbulence theory. part i: The concept of eddy-mixing across finite distances, *Journal of Atmospheric Sciences*, 41(23), 3351–3367.

Suselj, K., Kurowski, M. J., Teixeira, J. (2019), A unified eddy-diffusivity/mass-flux approach for modeling atmospheric convection, *Journal of the Atmospheric Sciences*, 76(8), 2505–2537.

Tiedtke, M. (1989), A comprehensive mass flux scheme for cumulus parameterization in large-scale models, *Mon. Wea. Rev.*, 117(8), 1179–1800.

Troen, I., Mahrt, L. (1986), A simple model of the atmospheric boundary layer; sensitivity to surface evaporation, *Boundary-Layer Meteorology*, 37(1-2), 129–148.

Villefranque, N., Blanco, S., Couvreux, F., Fournier, R., Gautrais, J., Hogan, R. J., Hourdin, F., Volodina, V., Williamson, D. (2021), Process-based climate model development harnessing machine learning: Iii. the representation of cumulus geometry and their 3d radiative effects, *Journal of Advances in Modeling Earth Systems*, 13(4), e2020MS002423.

von Salzen, K., McFarlane, N. A. (2002), Parameterization of the bulk effects of lateral and cloud-top entrainment in transient shallow cumulus clouds, *Journal of the atmospheric sciences*, 59(8), 1405–1430.

Yamada, T. (1983), Simulations of nocturnal drainage flows by a q2l turbulence closure model, *Journal of the Atmospheric Sciences*, 40(1), 91–106.

Yanai, M., Esbensen, S., Chu, J.-H. (1973), Determination of bulk properties of tropical cloud clusters from large-scale heat and moisture budgets, *Journal of Atmospheric Sciences*, 30(4), 611–627.

Zipser, E. (1977), Mesoscale and convective–scale downdrafts as distinct components of squall-line structure, *Monthly Weather Review*, 105(12), 1568–1589.